Trends in the types and absorption characteristics of ambient aerosols over the Indo-Gangetic Plain and North China Plain in last two decades

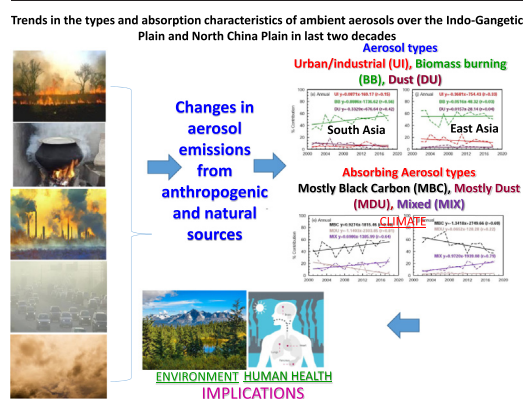S. Ramachandran [a,b,*], Maheswar Rupakheti [b]

[a] Physical Research Laboratory, Ahmedabad, India
[b] Institute for Advanced Sustainability Studies, Potsdam, Germany

HIGHLIGHTS

- First time, trends in aerosol types, absorbing aerosol types over Asia are analyzed.
- Biomass burning aerosol type exhibits a positive trend over South and East Asia.
- Urban/industrial aerosol type shows positive (negative) trend over South (East) Asia.
- Absorbing aerosol types (BC, dust and mix) show statistically significant trends.
- Changes in anthropogenic emissions reason for trends not natural or climatic factors.

GRAPHICAL ABSTRACT

ABSTRACT

The sixth assessment report released by the Intergovernmental Panel on Climate Change (IPCC) in 2021 states that our inadequate understanding of magnitudes and trends of atmospheric aerosols, particularly over Asia, is a major source of uncertainty in climate change. In this study, the climatology and trends in different types of aerosols with focus on absorbing aerosols over Kanpur located in the Indo-Gangetic Plain (IGP) in South Asia and Beijing in the North China Plain (NCP) in East Asia are derived for the first time. We perform a first analysis of high-quality time series of columnar aerosols observations over a period of nearly two-decades, along with satellite observations to provide a broader regional perspective. The satellite retrieved aerosol Ångström exponent (AE) values have increased (10–20%) suggesting an increasing contribution of fine aerosols to aerosol optical depth (AOD) over Asia in last 2-decades. Among the three aerosol types [urban-industrial (UI), biomass burning (BB), and dust (DU)], only UI and BB aerosols are present over Kanpur throughout the year, while DU is present along with UI and BB aerosols only during pre-monsoon and monsoon. Overall, there is a positive trend in BB aerosols over both Kanpur and Beijing, a positive (negative) trend in UI aerosols over Kanpur (Beijing), and positive (negative) trend in dust over Beijing (Kanpur). However, only the positive trend in BB aerosol type over Kanpur is statistically significant. Further, among the three absorbing aerosol types [mostly black carbon (MBC), mostly dust (MDU), and mixed (MIX) containing BC and dust], only MBC and MIX are present in post-monsoon and winter over IGP, and MDU is present along with MBC and MIX only during pre-monsoon and monsoon, which is in agreement with aerosol types found. Trends in MBC, MIX and MDU over Kanpur in IGP and in MIX over Beijing are statistically significant. These trends are attributed mainly to the changes in anthropogenic aerosol emissions, and not to natural and climatic factors as their changes are relatively small. These

* Corresponding author at: Physical Research Laboratory, Ahmedabad, India.
E-mail addresses: ram@prl.res.in srikanthan.ramachandran@iass-potsdam.de (S. Ramachandran).

findings on hitherto unavailable climatology and trends in aerosols and absorbing aerosols over two global aerosol hotspots and identified contrasts will be crucial in model simulations to better decipher the aerosol-climate interactions over Asia.

1. Introduction

The net global aerosol direct radiative effect on Earth's climate due to heating and cooling by aerosols is negative, which has masked a substantial portion of the warming due to well-mixed greenhouse gases (GHGs). For example, the increase in well-mixed GHGs led to a warming of 1°C to 2°C from 1850 to 1900 to 2010–2019 with aerosols contributing a cooling of 0.0°C to 0.8°C (IPCC, 2021). However, the annual -, global -mean temperature change due to aerosol radiative forcing (ARF) is uncertain by a factor of two (IPCC, 2021). The large uncertainty in estimation of aerosol impact on climate remains due to, among others, an inadequate understanding of magnitudes and trends of aerosols in Asia, a major aerosol source region (IPCC, 2021). Because of non-uniformity in ARF due to variations in sources and composition of aerosols across time and different locations, net aerosol effect on climate globally or regionally is not simply a fractional offset. One of the most crucial parameters that contributes to uncertainty in ARF estimates is the aerosol absorption, including columnar aerosol absorption, as its accurate measurements across different regions and seasons are lacking (IPCC, 2013; Hoegh-Guldberg et al., 2018). Several methods have been employed in past studies to distinguish different aerosol types and absorbing aerosol types using the columnar aerosol optical and microphysical properties. The relations between aerosol extinction Ångström exponent (EAE) and absorption Ångström exponent (AAE), EAE and single scattering albedo (SSA), and EAE and real part of refractive index (RRI) of aerosols are typically utilized to classify the aerosol types, while the absorbing aerosol types are classified utilizing the relations between fine mode fraction (FMF) in aerosol optical depth (AOD) and Ångström exponent (AE), FMF and SSA, and FMF and AAE (Russell et al., 2010, 2014; Giles et al., 2012; Kedia et al., 2014; Zheng et al., 2017; Rupakheti et al., 2019; Ramachandran and Rupakheti, 2020; Yang et al., 2021a). The spectral dependence of aerosol optical properties [optical depth (AE), extinction (EAE), and absorption (AAE)], physical properties (size – (FMF), and chemical properties (refractive index) help in separating the aerosols from different sources, regions and fuel types (Ramachandran and Rupakheti, 2020; Yang et al., 2021b). The aerosol types are classified as urban/industrial (UI) aerosols, biomass burning (BB) aerosols, and dust (DU). The aerosols over urban areas and industrialized regions are mainly from fossil fuel combustion and biomass burning in anthropogenic activities, and dominantly fine particles, whereas the coarse particles such as sea salt and dust particles, mostly from natural sources, are present as a function of season. It may be noted that sea salt aerosols can be important over coastal and oceanic sites, however, classifying them as pure sea salt has limitations because of their high SSA (~1) and small EAE values (due to larger size) (Russell et al., 2010, 2014). The absorbing aerosol types are categorized as mostly black carbon (MBC), i.e., a mixture of urban/industrial and biomass burning emissions with BC aerosols as the dominant absorbers, mostly dust (MDU), i.e., dust is the dominant absorber, and mixture (MIX), i.e., a mixture of fine mode BC particles and coarse mode dust particles as dominant absorbers (Giles et al., 2012; Ramachandran and Rupakheti, 2020).

Asia is a global aerosol hotspot. Aerosol emissions are changing rapidly over Asia, especially the anthropogenic emissions (Samset et al., 2019). The recent changes in aerosol emissions over Asia, with the emissions increasing over South Asia and decreasing over East Asia, have resulted in a dipole in aerosol pollution between South Asia and East Asia (Samset et al., 2019;

Ramachandran et al., 2020a). The current climate models with state-of-the-art representation of physical and chemical processes are yet found to grossly underestimate aerosol absorption in many regions, especially over Asia (Shindell et al., 2013; Myhre et al., 2017). The knowledge and information on the ground level aerosol pollution is of a crucial concern from air quality and public health perspective. The impact of air pollution on human health is a serious public health crisis across Asia, where around 92% of the region's population is exposed to particulate air pollution levels in excess of the World Health Organization (WHO) guidelines 2005 for protection of public health (UNEP, 2019). On local and global scales, identifying the factors that drive climate change, and that connect it to air pollution, is crucial to effectively reduce emissions and their impacts (Meng et al., 2019; UNEP, 2019). Aerosol emissions and their geographical distributions have changed considerably over the last decade in Asia as a result of growing economic activities in various regions and introductions of air pollution control regulations in Asian countries with a primary emphasis on reducing adverse impacts of air pollution on public health (Meng et al., 2019). AOD and SSA vary depending on the environmental setting, sources, meteorological conditions (relative humidity, winds, planetary boundary layer (PBL), rainfall, solar radiation) and dynamics (horizontal and vertical transport), and from season to season. For example, weather conditions such as high wind speeds, low relative humidity, higher PBL heights, rainfall could favor an early dispersion of pollutants whereas weather conditions otherwise (low wind speeds, higher relative humidity, lower PBL heights, less rainfall) may further worsen the air pollution (e.g., Li et al., 2020). Air quality is not only a primary public health concern but is equally important in the context of aerosol-climate interaction as the size and composition of particles present can influence the physical, optical and chemical properties of aerosols (e.g., AOD and SSA).

The columnar aerosol properties including the aerosol type and absorbing aerosol type play a pivotal role in determining the weather, radiative and climate impacts (Ramachandran et al., 2020a; Zhao et al., 2020). The trends in aerosol impact on climate and climate change including the changes in precipitation and hydrological cycle based on model simulated aerosol absorption characteristics over these regions may not be very precise given the uncertainties associated and limitations of models including aerosol absorption (e.g., Shindell et al., 2013; Myhre et al., 2013; Ramachandran et al., 2020a, 2020b), rapidly changing aerosol emissions in the region, and the non-availability of observation-based trend analysis. This is vital since the radiative and climate effects that result from the recent changing aerosol patterns, especially decreasing emissions since 2013 in China (Fan et al., 2020), are expected to be different from those observed earlier (Samset et al., 2019). These changes can potently turn on large scale atmospheric responses with wide-ranging impacts on climate, clouds, chemistry, and other atmospheric processes extending well beyond the source regions of aerosols and their precursors in South and East Asia (Samset et al., 2019). Thus, we investigate the climatology and derive the trends in seasonal and annual time series of aerosol types (UI, BB, DU) and absorbing aerosol types (MBC, MDU, MIX) hitherto unavailable over two major global aerosol hotspot regions, South and East Asia. In doing so we utilized the high-quality time series of observations over a period of two-decades of the radiative- and climate-relevant columnar aerosol characteristics over Kanpur in South Asia and Beijing in East Asia, along with satellite observations providing a broader regional perspective (Fig. 1).

Fig. 1. Satellite retrieved aerosol Ångström exponent (AE) over Asia: The AE data were obtained using the MODIS Terra Deep Blue version 6.1 level-3 daily mean for Land. Seasonal changes in AE over Asia for 2001-05, 2014-18 and the difference between the time two periods ((2014-18)–(2001-05)) corresponding to (a) winter, (b) pre-monsoon, (c) monsoon, (d) post-monsoon seasons and on (e) Annual scale.
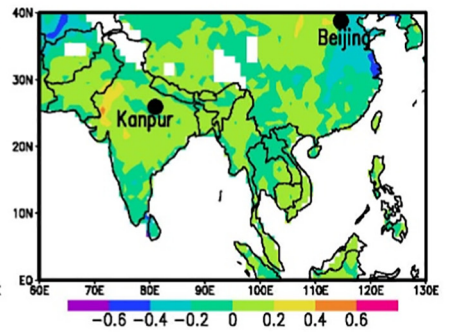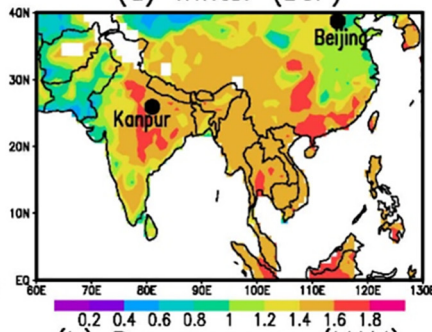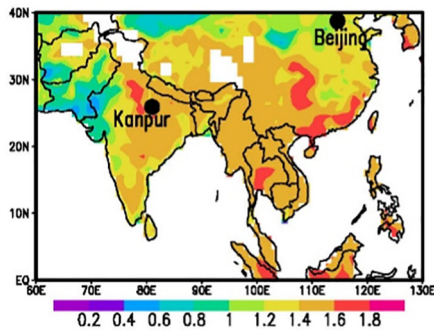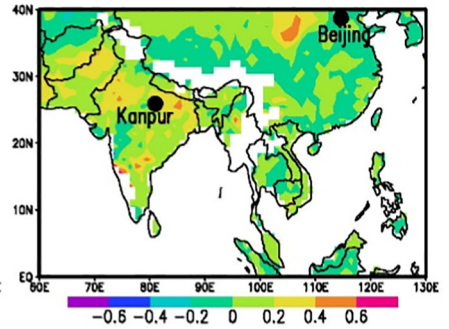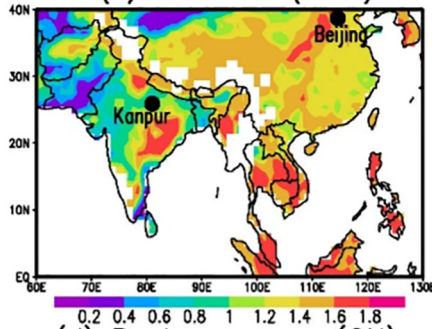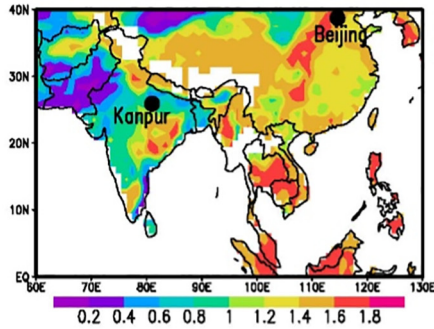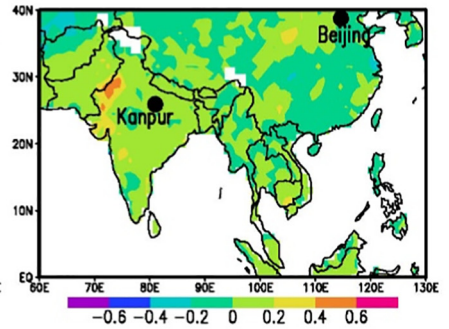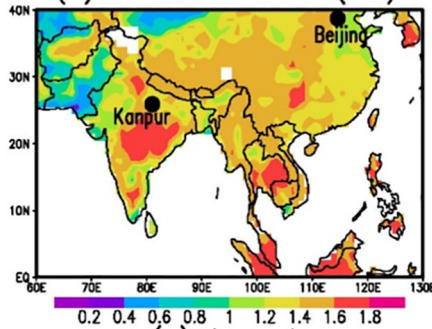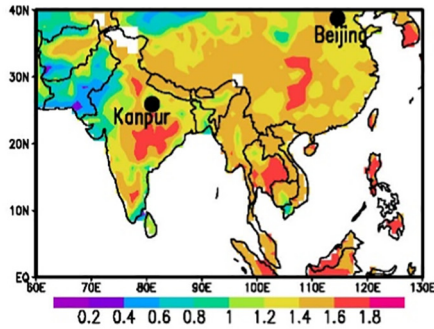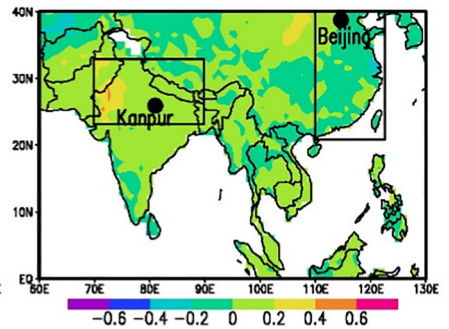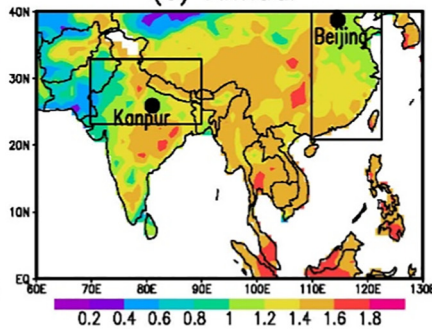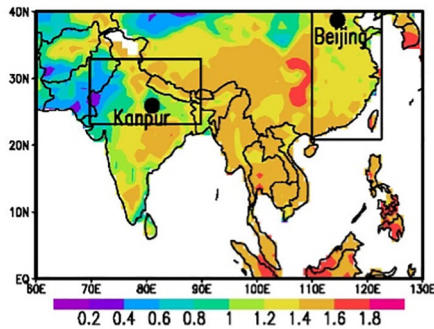
2. Data and methodology
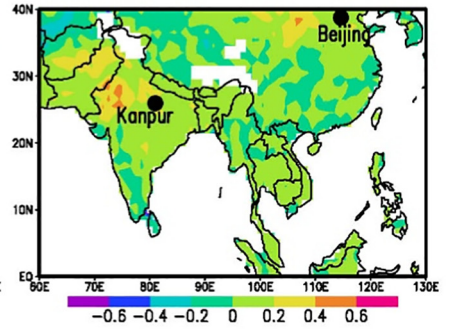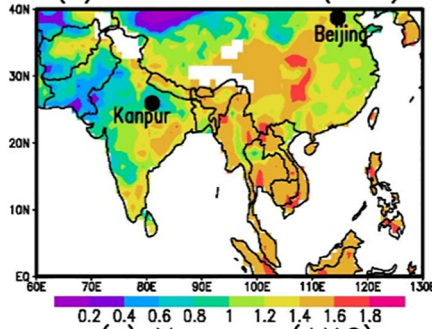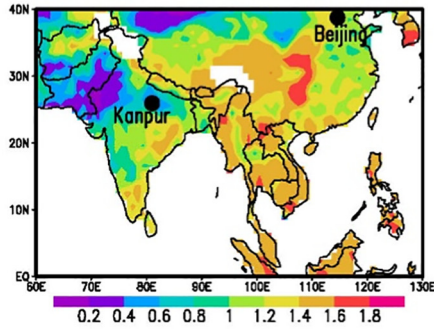
2.1. Study region and measurement sites

The two aerosol robotic network (AERONET) (https://aeronet.gsfc.nasa.gov/) sites - Kanpur (26.5°N, 80.2°E, 123 m above mean sea level (asl)) in the Indo-Gangetic Plain (IGP) in South Asia and Beijing (39.9°N, 116.4°E, 92 m asl) in the North China Plain (NCP) in East Asia are shown in Fig. 1. Kanpur is located ca. 500 km downwind of Delhi, a megacity with 30 million inhabitants. Kanpur is a densely populated (ca. 3 million inhabitants), industrialized and heavily polluted location. Beijing, a megacity with a population of 20 million, is located in the heavily industrialized and highly polluted NCP. The general environmental ambience of the sites, and the aerosol characteristics are very similar over Beijing and Kanpur (Eck et al., 2010; Ramachandran et al., 2020a). They are urban areas where emissions from fossil fuel combustion and biomass burning occur during all seasons, along with desert dust events that occur primarily in the pre-monsoon (spring) season (March–May) which contribute to the heavy aerosol pollution (Eck et al., 2010). Over India and China, fossil fuels (coal, oil and natural gas) contribute 70% or more to the primary energy supply, and their contribution is rather steady during the last 2-decades (Ramachandran et al., 2022). BC emissions in China are at least twice as high as in India (Kurokawa and Ohara, 2020). BC emissions in China continued to increase from early 2000s to 2010 and then started to fall mainly due to reductions in transport and industrial emissions rapidly and a slight decrease in residential emissions (Kurokawa and Ohara, 2020; Kanaya et al., 2020). The reductions in residential emissions were mainly caused by a decrease in emissions from biomass consumption (Kurokawa and Ohara, 2020). In contrast, in India BC emissions showed increasing trends during the last 2-decades caused by growth of emissions from diesel vehicles and industrial sector (Kurokawa and Ohara, 2020). Both sites are heavily influenced by regional emissions, in addition to emissions from their own local sources. The plains in South Asia (IGP) and East Asia (NCP) are influenced by the dynamics of Asian summer monsoon with northeasterly and southwesterly winds during the winter and summer monsoon seasons, respectively. Over both the areas the monsoon period is June–September, during which ≥80% of the total annual rainfall occurs. In general, across India the aerosol emission types (from fossil fuel and biomass burning, and dust) were found to be the same throughout the year (Kedia et al., 2014; Ramachandran et al., 2015), which holds good for the IGP too. However, the abundance of each aerosol type varied across the region (depending on urban, remote, continental and rural) and seasons (winter, monsoon) (Ramachandran et al., 2015). Across China, including Beijing the aerosol types were found to be the same as over the IGP, however, their abundances exhibited different proportions depending on the locales (urban, rural and coastal) (Che et al., 2019). Further, during wintertime both IGP and NCP are found influenced by severe haze/fog events (Ramachandran et al., 2015; An et al., 2019; Che et al., 2019).

2.2. Satellite observations over Asia

The MODIS Terra version 6.1 daily level-3 Å Exponent (AE) data (https://giovanni.gsfc.nasa.gov/giovanni/) are utilized. AE, a spectral derivative of aerosol optical depth (AOD), is derived using the AODs retrieved in the 0.47 μm–0.65 μm wavelength range in MODIS Terra Deep Blue Algorithm (Sayer et al., 2019). The uncertainty in MODIS Terra AOD is ±0.05 ± 0.15AOD over land (Levy et al., 2013). AE is used widely to quantify whether the fine mode or coarse mode aerosols are dominant in the column as AE depends on the aerosol size distribution. AE values are in the range of 1 to 3 when dominated by fine mode aerosols (e.g., combustion aerosols) in the accumulation mode whereas smaller AE values (~zero) occur when the aerosol size distribution is dominated by coarse mode aerosols (dust and sea salt) (e.g., Eck et al., 2010; Kedia et al., 2014). Further, it should be noted that either an increase in the number of smaller particles or a decrease in the number of bigger particles in the size distribution can cause an increase in the AE values. Annual and seasonal averages (Fig. 1) of AE

corresponding to two 5-year periods, 2001–2005 (the beginning of the study period) and 2014–2018 (the end of the study period), are compared to prevent any biases and features that can arise out of inter-annual variability.

2.3. Ground-based measurements of columnar aerosol parameters

The extinction Ångström exponent (EAE), real part of refractive index (RIR), Ångström exponent (AE), fine mode fraction (FMF) and the linear depolarization ratio (LDR) retrieved from measurements with the sun/sky radiometers at the AERONET sites at Kanpur and Beijing are analyzed to obtain a hitherto unavailable regional and seasonal description of climatology and trends in aerosol types and absorbing aerosol types over South and East Asia. The level 2, version 3 cloud-screened and quality-assured daily data retrieved from direct and solar almucantar inversion algorithm are utilized. The ground-based Sun-sky radiometers measure direct solar and diffuse sky radiances in the spectral range of 0.34–1.02 μm (Holben et al., 2001). The radiometer, which has a field of view of 1.2°, makes direct solar radiation measurements roughly every 15 min under clear sky condition. For direct solar measurement, triplet observations are made at each wavelength for calibration (using Langley technique) and to screen the clouds (Holben et al., 2001). In the present study, the direct solar measurements made at four spectral channels (0.44, 0.50, 0.675 and 0.87 μm) and the sky radiance measurements made at four spectral channels (0.44, 0.675, 0.87 and 1.02 μm) are utilized. The radiometers under AERONET are calibrated routinely (approximately every six to twelve months) following a detailed procedure so as to ensure data continuity and measurement quality (Dubovik et al., 2000; Holben et al., 2001). The data for the period of 2001–2018 over Kanpur and Beijing are utilized. The duration of level 2 data availability is the longest over Kanpur and Beijing than any other site (s) throughout South Asia and East Asia, respectively. The above data were available only for 3 months during 2001 (Mar-May), and 2005 (Oct-Dec) over Beijing and hence the data from these years are not included in the analysis. The seasonal and annual averages are calculated from the daily-average of instantaneous aerosol properties measured at 20 min time interval with typically about 15 measurements each day during the chosen year (s). The seasons are defined as winter (December–January-February (DJF)), pre-monsoon or spring (March–April-May (MAM)), monsoon (Jun-July-August-September (JJAS)) and post-monsoon (October–November (ON)). The study region experiences overcast and cloudy conditions during the monsoon season reducing the number of data points due to cloud screening, however, the retrieved aerosol characteristics can be relied upon and are included because the observations during the monsoon also undergo the same level of quality control measures similar to the other seasons.

It should be noted that we have used version 3, level 2, quality-controlled, cloud-screened and calibrated AERONET data, and therefore uncertainties in these parameters are not expected to change any conclusions of the study. The uncertainties in the AERONET data and details of quality checks undertaken are briefly mentioned here. The uncertainty in AOD depends on wavelength; it is less than ±0.01 for wavelengths >0.44 μm and is less than ±0.02 for shorter wavelengths (Holben et al., 2001). The spectral AOD and extinction AOD (EAOD) follow a power law of the form $y = K\lambda^{-\alpha}$, where λ is the wavelength, y is AOD or EAOD, and α is AE or EAE, respectively. AE, and EAE are derived using AOD, and EAOD, measured at 0.44, 0.675 and 0.87 μm, respectively by least squares fitting of AOD or EAOD with respect to wavelength on a log-log plot. In principle, the AOD and EAOD are the same as both represent the columnar extinction/attenuation of radiation by aerosols, however, they are retrieved using two different algorithms in AERONET. For example, AOD is derived from the direct radiation measurements (direct sun algorithm) while EAOD is retrieved from the direct and diffuse sky radiation measurements (solar almucantar scenario in Inversion algorithm) (Dubovik et al., 2000). The error in the real part of refractive index (RIR) corresponding to the wavelength of 0.44 μm, which is used in the study, lies in the range of 0.025–0.05 (Dubovik et al., 2000). The fine mode fraction (FMF) is derived as the ratio of fine mode AOD (particles in the 0.01–1.0 μm radius range) to

total AOD (all the particles in 0.01–10 μm radius range) at 0.50 μm from the sky radiance measurements. The error in AERONET derived FMF is ~10% (O'Neill et al., 2003). The errors in the retrieved volume size distributions are not significant, and are found to not significantly affect the main features of the aerosol size distribution, namely, the concentration and effective radii (Dubovik et al., 2002). The linear depolarization ratio (LDR) corresponding to 0.532 μm wavelength is used. The AERONET retrieved aerosol parameters are reported to have the highest accuracy when solar zenith angle is between 50° and 80° (Dubovik et al., 2000); only those data that are within this solar zenith angle range are utilized in the present study.

2.4. Determination of aerosol type, and absorbing aerosol type

The suite of aerosol characteristics retrieved by AERONET and their inter-relation (EAE vs. RIR) can be used to classify aerosols into different source types, such as, originating from biomass burning, urban/industrial mix, and dust (Russell et al., 2010, 2014; Giles et al., 2012; Rupakheti et al., 2019). EAE represents the wavelength dependence of aerosol extinction, which is based on aerosol size distribution and varies depending on aerosol type and dominance (Russell et al., 2014). The RIR, which depends on the chemical composition of aerosols, defines the scattering contribution. The boundary values of EAE and RIR used to classify the different aerosol sources are EAE: 0.70–1.74 and RIR: 1.35–1.43 for urban/industrial (UI), and EAE: 1.00–1.50 and RIR: 1.43–1.57 for biomass burning (BB), and EAE: 0.01–0.41 and RIR: 1.44–1.59 for dust (DU) (Russell et al., 2014; Rupakheti et al., 2019). It is worth noting that the parameters EAE and RIR correspond to the total (composite) aerosols, as opposed to, for example, the relation between EAE and AAE (absorption Ångström exponent, the wavelength exponent derived from the spectral dependence of absorption AOD, i.e., AAOD). In addition, the threshold values for EAE and RIR that are used to classify the aerosols as UI, BB and DU type do not overlap unlike between EAE and AAE. The boundary values in case of relation between EAE and AAE are EAE: 0.80–1.60 and AAE: 0.60–1.30 for UI, and EAE: 0.80–1.70 and AAE: 1.10–2.30 for BB, and EAE: 0.01–0.40 and AAE: 1.00–3.00 for DU where the thresholds overlap.

The different absorbing aerosol types can be identified by utilizing the relation between AE and FMF. The AE is measure of the spectral dependence of AOD with the dominant sizes of aerosol size distribution, and enables to classify the absorbing aerosol types under three major categories as Mostly BC (MBC), Mostly Dust (MDU) and Mixed (as stated earlier) (Giles et al., 2012). The threshold limits used for the classification are AE: 1.00–1.50 and FMF: 0.70–1.00 for MBC, AE: 0.00–0.40 and FMF: 0.10–0.40 for MDU, AE: 0.40–1.00 and FMF: 0.40–0.70 for Mixed. In this classification also, both the parameters (AE and FMF) used to classify the absorbing aerosol types pertain to total (composite) aerosols, and the threshold limits do not overlap, unlike for example in case of AAE vs. FMF - AAE: 1.00–2.00 and FMF: 0.50–1.00 for MBC, AAE: 2.00–3.00 and FMF: 0.10–0.30 for MDU, and AAE: 1.00–2.00 and FMF: 0.17–0.40 for Mixed (Giles et al., 2012; Rupakheti et al., 2019). The light absorption by the other absorbing aerosol species, namely the brown carbon (BrC) is strongly wavelength dependent. The absorption by BrC is significantly lower (5-times) than that of BC. The BrC absorption is effective only over a narrow wavelength band in the 0.3 to 0.6 μm wavelength range and peaks around 0.37 μm, with its absorption falling very steeply beyond 0.4 μm, and makes a < 5% contribution to total light absorption beyond 0.55 μm (Kirillova et al., 2016). The role and influence of BrC in light absorption in this study is not included owing to the above, and due to the fact in the present study the classification into different aerosol types and absorbing aerosol types is based on composite (or total) aerosols and not on absorption AOD (Ramachandran et al., 2020b) which is needed to estimate the influence of BrC on light-absorption. Further, a comprehensive analysis of contribution of BC and BrC to AAODs over South and East Asia revealed that BrC contributes ≤ 25% to aerosol absorption over South Asia and ≤ 16% over East Asia (Ramachandran et al., 2020b).

2.5. Derivation of trends

The seasonal and annual trends on aerosol types and absorbing aerosol types are calculated using linear regression method. The linear regression method is simple, robust, and less sensitive to breaks in the time series of data, and thus, widely used to derive the trends in the time series of time-dependent geographical variables. In addition, the linear regression method is appropriate when the uncertainty in data is constant (i.e., residuals are Gaussian white noise). In this approach regression can be obtained by assigning the same precision for each parameter (or in other words allocating a weight of unity to each parameter). The statistical significance of the trends was tested and *p*-values at 95% confidence level (CL) are reported.

3. Results and discussion

3.1. Satellite observations of Ångström exponent

In general, satellite observations clearly show higher AE over the NCP than the IGP (Fig. 1), indicating the higher dominance of fine mode aerosols over East Asia. Higher AE results from dominance of fine mode aerosols in the aerosol size distribution whereas lower AE occurs when it is dominated by larger aerosols. Across the IGP and NCP the average AE during 2014–2018 is higher than during 2001–2005, indicating that the fine mode aerosols have increased relative to coarse mode aerosols in the last 2-decades. AE values exhibit significant seasonal variations in addition to spatial variations (Fig. 1). AE over India and the IGP are higher during winter and post-monsoon (>1) than during the pre-monsoon and monsoon seasons (<1); typically, during post-monsoon and winter fine mode aerosol emissions from anthropogenic activities dominate the aerosol distribution leading to higher AE whereas pre-monsoon and monsoon AE values are modulated by the coarse mode dust and sea salt particles resulting in lower AE (Kedia et al., 2014; Ramachandran et al., 2015). Over NCP seasonal variations in AE are less prominent (Fig. 1), with AE values in the 1.0 to 1.5 range during the year. The seasonal features in AE are similar in both the decades. The differences in average AE between 2014–2018 and 2001–2005 are positive and are in the range of 0.2 to 0.4 on a regional scale across the IGP and the NCP. Interestingly the AE values have become higher during pre-monsoon and monsoon seasons over the IGP during 2014–2018 compared to 2001–2005 period resulting in more positive differences suggesting that the fine mode aerosols have increased in these two seasons during the current decade. A seasonal trend analysis of AOD showed that natural aerosols mainly in the coarse mode (dust and sea salt) did not change enough to alter the AOD and SSA significantly across the seasons over the IGP, and the NCP during the last two decades. Thus, the changes or trends in AOD and SSA occurred/are controlled mainly due to/by the increase/decrease in emissions of anthropogenic aerosols (and aerosol precursor gases) (Ramachandran et al., 2020a) which are predominantly in the fine mode.

Trends in AE derived from MODIS data for both IGP and NCP as well as over Kanpur and Beijing for the 2001–2018 period are similar; the trends being statistically significant over Kanpur and IGP (Fig. 2). The positive (i.e., increasing AE) trends in AE during 2001–2018 over Kanpur and IGP are robust – they are statistically significant at 95% confidence level. In contrast, AE shows a slight negative trend over Beijing and NCP (Fig. 2) which however is not statistically significant. On the year-on-year comparison, the AE has increased in 2018 when compared to 2001, however, AE values start decreasing over Beijing and NCP post 2010 (Fig. 2). As the 2018 AE values are lower than the 2010 values the negative trends in AE, which are negligible and not statistically significant, are observed over Beijing and the NCP. It can be attributed to the reduction in AOD due to reduction in emissions of primary aerosols and aerosol precursor gases as a result of comprehensive emission controls in China during the recent decade (2010–2017) (Ramachandran et al., 2020a). The ± 1σ (standard deviation) from the mean (vertical bars) in the area-averaged AE decreases in the more recent years (Fig. 2) indicating a regional homogeneity in increase or decrease in
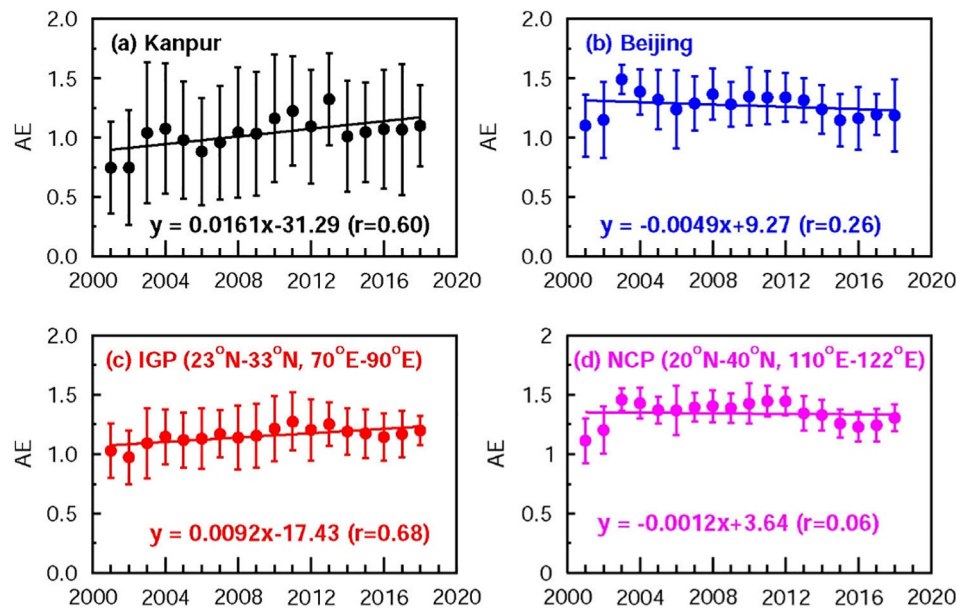
Fig. 2. Trend in satellite retrieved Ångström exponent (AE) over South and East Asia: (a) Kanpur (*p*-value <0.01, significance <0.01 at 95% confidence level (CL)), and (b) Beijing (p-value 0.25, significance 0.30 at 95% CL), (c) South Asia (p-value <0.01, significance <0.01 at 95% CL) and East Asia (p-value 0.69, significance 0.80 at 95% CL). The AE values in (c) and (d) are averaged over the areas as shown in boxes in Fig. 1.

emissions of aerosols and their precursors. The variations in the standard deviations of AE over IGP and NCP are attributed primarily to the differences in the amounts, and changes in aerosol emissions (Zheng et al., 2018; Li et al., 2017; Fan et al., 2020) rather than due to inter-annual change in meteorological condition as the effects due to inter-annual meteorological variations on aerosol concentrations during 2013–2017 were found to be relatively small (Zhang et al., 2019). Another notable feature in trends is evident between the two regions – the rate of increase in AE is higher at local scale (Kanpur) in South Asia when compared to the broader IGP region (Fig. 2a, c), similarly over East Asia the rate of decrease is lower over NCP compared to Beijing (Fig. 2b, d). Thus, the results indicate that though there are differences in the magnitudes of rate of increase/decrease on regional (IGP, NCP) and local scales (Kanpur, Beijing), based on the overall similarity in aerosol parameters (discussed in Section 2.1) and their trends, aerosol characteristics measured at these two individual locations can be made use of as being broadly representative of the respective region of their location.

3.2. Aerosol optical characteristics, aerosol type and absorbing aerosol type over Kanpur and Beijing

3.2.1. Aerosol optical characteristics

The AE, EAE, RIR and FMF all exhibit seasonal variations (Fig. 3). At the outset, the Beijing values are higher than Kanpur. EAE and AE are values are almost same. They are lowest during pre-monsoon over both the locations (<1 over Beijing, and ≤ 0.6 over Kanpur). Over Kanpur, EAE and AE values are lower (~0.6) even in monsoon while such a decrease in EAE and AE are not clearly evident over Beijing. Lower EAE and AE values arise due to the increase in the amount of bigger size particles in the aerosol size distribution. In the pre-monsoon season in South and East Asia, the winds that travel through the upwind arid regions to the west (e.g., Thar, Taklimakan, Arabian Peninsula) bring in desert dust (coarse) particles to the Indo-Gangetic Plain (IGP) and the North China Plain (NCP) (Kedia et al., 2014; Che et al., 2019) thereby reducing the AE. During monsoon season dust and sea salt particles contribute to aerosol distribution over the IGP (Kedia et al., 2014; Ramachandran et al., 2015), resulting in lower AE and EAE values. The winter and post-monsoon seasons over the IGP and the NCP are dominated by fine mode aerosols from fossil fuel and biomass burning emissions (Kedia et al., 2014; Ramachandran et al., 2015; Jethva
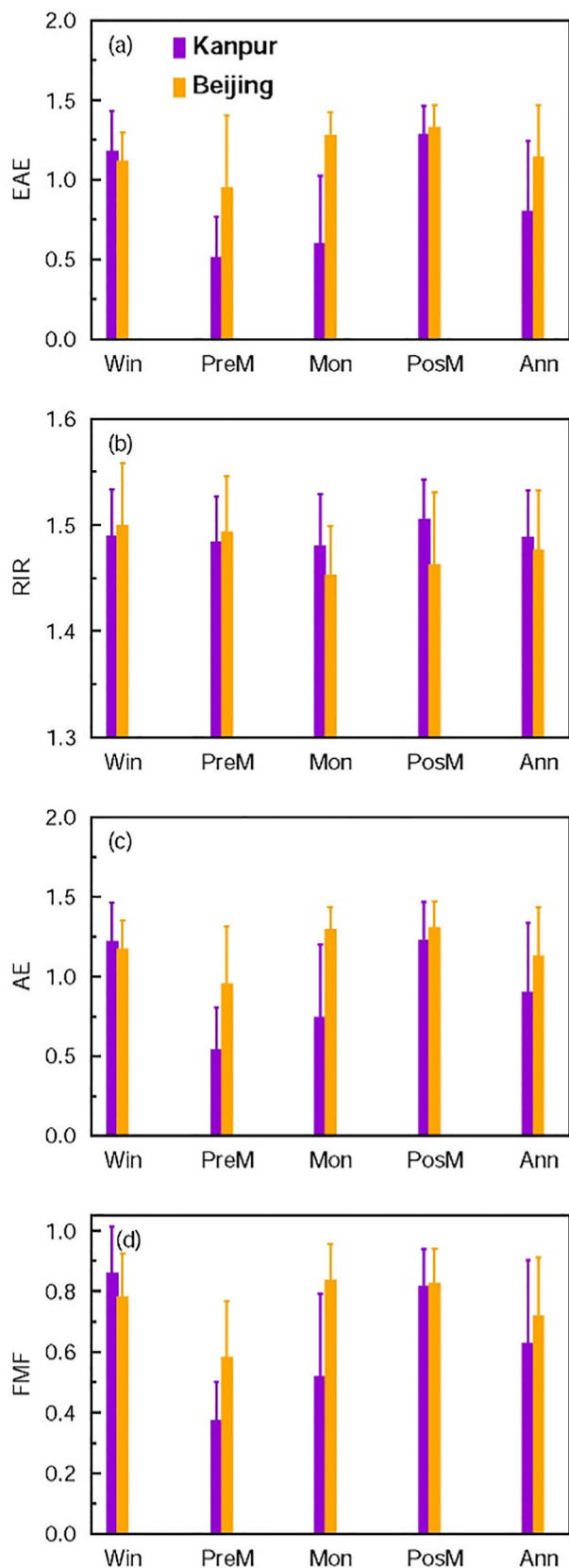
et al., 2019; Che et al., 2019) giving rise to AE values higher than 1. The seasonal variation of FMF follows that of AE and EAE. FMF is lowest during pre-monsoon over Kanpur (<0.4) and Beijing (<0.6), and it is about 0.5 over Kanpur during monsoon. Aerosols in fine mode dominate the aerosol distribution during post-monsoon and winter (FMF ≥ 0.8). The RIR is around 1.50. It has the least variation during the year over both South and East Asia. RIR values over Kanpur and Beijing are comparable during winter and pre-monsoon. RIR values are lower over Beijing than Kanpur during monsoon and post-monsoon. The RIR was found to lie in the 1.40–1.47 range for urban/industrial and mixed aerosols, 1.47–1.52 range for biomass burning aerosols and 1.36–1.56 range for desert dust (Dubovik et al., 2002). The RIR over Kanpur is >1.49 during post-monsoon and winter when the aerosols from biomass burning and urban/industrial emissions dominate, and decreases during pre-monsoon and monsoon when dust and sea salt aerosols also contribute to the aerosol distribution, which are consistent with the range of RIR reported for different environmental settings. Similar features are seen over Beijing – RIR is higher during winter and post-monsoon than in the monsoon season.

3.2.2. Aerosol types

The aerosol types and absorbing aerosol types over Kanpur (IGP) and Beijing (NCP) follow the seasonal variations in aerosol physical and chemical characteristics (Fig. 4). UI and BB types are present throughout the year in all seasons over both the locations. Dust (DU) type is present only during pre-monsoon and monsoon over Kanpur, and only during pre-monsoon over Beijing (Fig. 4). BB is the largest aerosol type in Kanpur during post-monsoon (ca. 80%) and winter (ca. 60%) while DU is a major aerosol type (40–50%) in pre-monsoon and monsoon. The dominance of BB aerosol type during post-monsoon over the IGP occurs due to the transport of intense crop residue burning emissions over northwestern IGP (Ramachandran et al., 2015; Jethva et al., 2019). These results on aerosol type over Kanpur are consistent with earlier results (e.g., Kedia et al., 2014; Ramachandran et al., 2015; Jethva et al., 2019).

Over Beijing, the contribution of UI aerosol type increases gradually from winter (8%) to post-monsoon (56%) whereas the BB aerosol type reduces gradually during the same timeframe, with BB being the dominant aerosol type. Dust aerosols with light-absorbing properties were found to occur more frequently in spring (pre-monsoon) over northeastern China than in the more southern regions (Zhao et al., 2015). The two major causes

that influence the aerosol chemical composition between northern and southern China were found to be the variations in anthropogenic emissions from seasonal biomass burning and residential heating (Che et al., 2018).

Fig. 3. Aerosol characteristics over Kanpur and Beijing derived from the AERONET observations: seasonal mean (Win: winter, PreM: pre-monsoon, Mon: monsoon and PosM: post-monsoon) and annual (Ann) values of (a) extinction Ångström exponent (EAE), (b) real part of refractive index (RIR), (c) Ångström exponent (AE), and (d) fine mode fraction (FMF) over Kanpur and Beijing in 2012 and 2011, respectively. The vertical bar in each column represents ±1σ (standard deviation) from the seasonal or annual mean.

High percentage of absorbing aerosols found at the northeastern sites, during winter, were more likely due to emissions of carbonaceous aerosol from residential heating (Zhao et al., 2015). The prevailing meteorological conditions over northern China during winter when the winds are mainly from the north and northwest, and during pre-monsoon when the winds are from the south and southwest influence aerosol characteristics in different regions of China (Xie et al., 2020). The findings from the current study on the aerosol types over Beijing are consistent with these results on columnar aerosol characteristics (e.g., Che et al., 2019) as well as the results on surface aerosol chemical composition contribution of biomass burning to fine particulate matter and BC (e.g., Xie et al., 2020). Residential heating in cold seasons (late autumn–winter–early spring) is mostly related to coal combustion in northern China, while over rural regions biomass burning is also used for heating. Furthermore, open biomass burning is also popular and widespread during harvest season. It was found that the influence of coarse particle (dust) was limited during the other seasons than pre-monsoon (Xie et al., 2020) similar to our results.

3.2.3. Absorbing aerosol types

The absorbing aerosol types over Kanpur and Beijing validate the observed aerosol types (Fig. 4g, h). During post-monsoon and winter the dominant absorbing aerosol type (≥70%) over Kanpur is MBC which drops very significantly to 2% during pre-monsoon. The aerosol absorption by MBC primarily occurs over Kanpur due to the combination of aerosol sources, the prevailing meteorological conditions and atmospheric transport. The post-monsoon season is marked by the emissions from the crop residue burning over northwestern India and their transport across the IGP which exhibits a spatial gradient (Kedia et al., 2014; Jethva et al., 2019). The winds over IGP are calm and northerly or northwesterly during post-monsoon (Ramachandran et al., 2015). The winter is marked by colder temperatures over the IGP. The shallow planetary boundary layer and the increase in anthropogenic emissions in addition to vehicular/industrial emissions, due to biomass burning (residential heating) results in more amount of BC over IGP (Kedia et al., 2014; Ramachandran et al., 2015). In pre-monsoon the aerosol absorption is mainly due to MDU and MIX type aerosols. In contrast during monsoon it is due to MBC and MDU and a small fraction by MIX aerosols. As seen earlier in aerosol type, MDU as an absorbing aerosol type is present only during pre-monsoon and monsoon (Fig. 4). MBC is the dominant absorbing aerosol type (≥70%) over Beijing during winter, monsoon and post-monsoon whereas all the three absorbing aerosol types are present during pre-monsoon (Fig. 4). The source of BC in Beijing is found to be dominantly from local traffic emissions in pre-monsoon while emissions from coal combustion and biomass burning were also important during winter (Zhao et al., 2015; Xie et al., 2020). Further, dust was found to be important for aerosol absorption during pre-monsoon (e.g., Xie et al., 2020), similar to our results (Fig. 4).

The presence of different aerosol types and absorbing aerosol types during the year with different proportions over Kanpur in South Asia and Beijing in East Asia are in contrast to the results obtained over Hanimaadhoo, a coastal site in the Indian Ocean affected largely by South Asian pollution outflow during dry season, where the absorbing aerosol types were MBC and MIX type during winter, pre-monsoon and post-monsoon, while MDU was the most dominant and contributed >95% to aerosol absorption during monsoon (Ramachandran and Rupakheti, 2020). Results on aerosol types and absorbing aerosol types over Kanpur in the current study are consistent with results from earlier studies over IGP (e.g., Kedia et al., 2014). Over Gandhi College, a rural location, ~500 km downwind of Kanpur in the central IGP, MDU absorbing aerosol type was absent throughout the year as
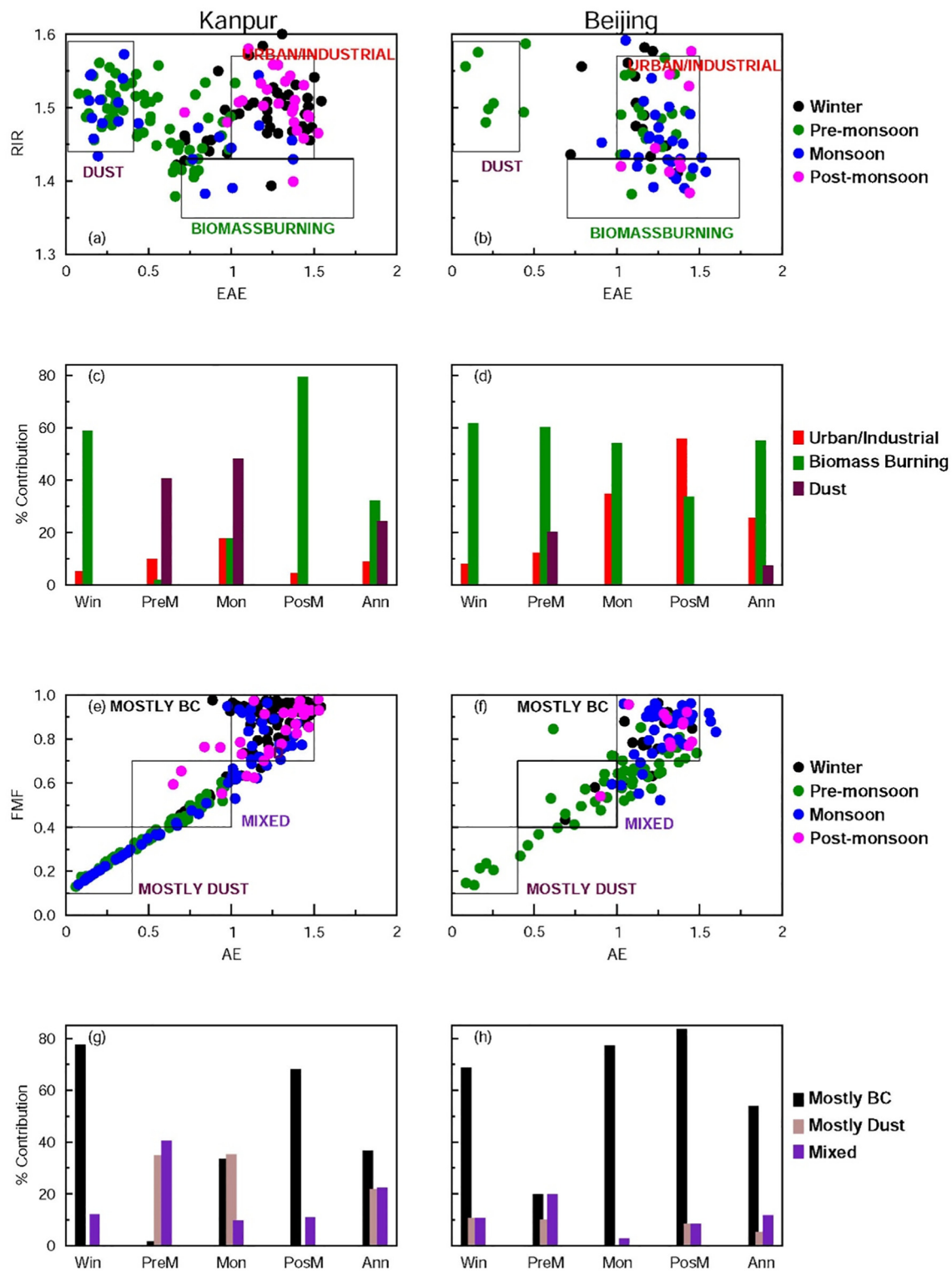
Fig. 4. Aerosol types [classified as Urban/Industrial (UI), Biomass Burning (BB) and Dust (DU)] and absorbing aerosol types [classified as (Mostly BC (MBC), Mostly Dust (MDU) and Mixed (MIX)] derived from the AERONET observations over Kanpur and Beijing in different seasons (Win: winter, PreM: pre-monsoon, Mon: monsoon and PosM: post-monsoon) and annual (Ann) scales: aerosol types over (a) Kanpur in 2012 and (b) Beijing in 2011, percentage contributions of aerosol types over (c) Kanpur and (d) Beijing, absorbing aerosol types over (e) Kanpur in 2012 and (f) Beijing in 2011, and percentage contributions of absorbing aerosol types over (g) Kanpur and (h) Beijing.

dust exhibits a west (high) to east (low) gradient across the IGP (Ramachandran et al., 2015). Similar to Gandhi College, MBC and MIX aerosols were present in all the seasons while MDU was absent in Lumbini (located in the northern edge of the central IGP, ca. 400 km to the northeast from Kanpur) and Kathmandu (a polluted valley in the foothills of central Himalaya, ca. 600 km to the northeast from Kanpur) (Rupakheti et al., 2019). It should be noted that the results mentioned above in comparison follow the same approach (boundary values/thresholds for the different aerosol characteristics and the seasonality are the same) outlined in the present study to classify and categorize the aerosol type and the absorbing
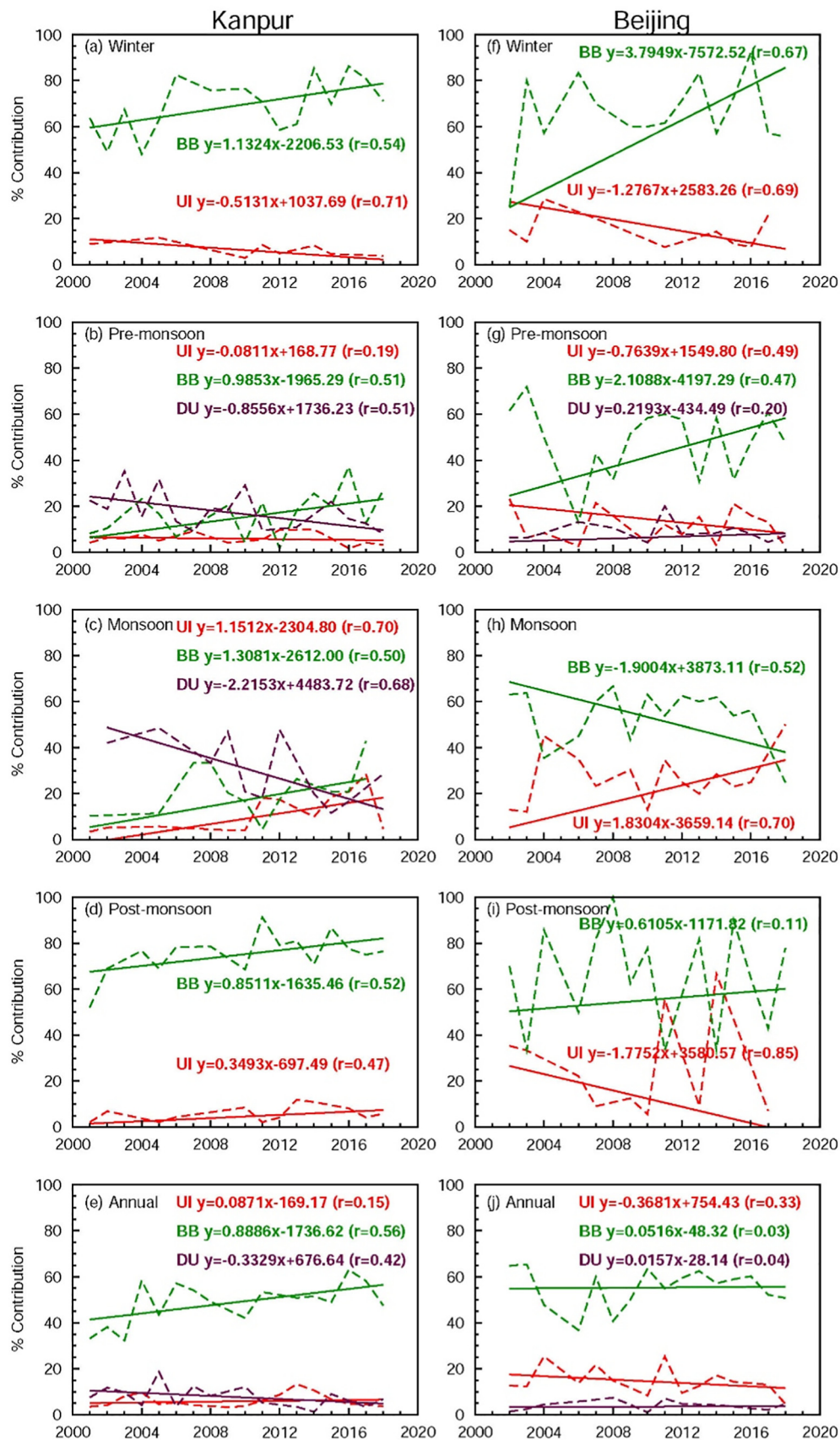
Fig. 5. Seasonal and annual trends in aerosol types [urban/industrial (UI), biomass burning (BB) and dust (du)] derived from the AERONET observations over Kanpur and Beijing during 2001–2018: Left column for Kanpur [(a) winter, (b) pre-monsoon, (c) monsoon, (d) post-monsoon, and (e) annual], and right column for Beijing [(f) winter, (g) pre-monsoon, (h) monsoon, (i) post-monsoon, and (j) annual]. The equations for the overall trend (2001–2018) for each aerosol type are given in each figure.

Table 1

Details of statistical tests (*p*-values at 95% confidence level) for the trends in different aerosol types [urban/industrial (UI), biomass burning (BB) and dust (DU)] over Kanpur and Beijing on seasonal and annual scales. Trends in linear depolarization ratio (LDR) are also given. The p-values ≤0.05 are shown in boldface.

Season	Kanpur				Beijing			
	UI	BB	DU	LDR	UI	BB	DU	LDR
Winter	**0.02**	**0.03**		0.67	**0.05**	**0.01**		0.94
Pre-monsoon	0.50	**0.04**	**0.03**	0.10	0.10	0.09	0.44	0.42
Monsoon	**<0.01**	**0.05**	**0.01**	**0.02**	**<0.01**	**0.04**		0.43
Post-monsoon	0.07	**0.05**		0.08	**<0.01**	0.70		0.88
Annual	0.58	**0.03**	0.10	0.38	0.20	0.95	0.90	0.21

aerosol type. A seasonal classification of aerosol type and absorbing aerosol type is important to distinguish the natural from anthropogenic aerosols. Further, in order to quantify the aerosol absorption which has implications to radiation budget and climate, we need to critically investigate and examine the climatology of aerosol types and absorbing aerosol types with an aim to determine whether they maintain the same seasonal variations every year.

3.3. Climatology and trends in aerosol type and absorbing aerosol type over Kanpur and Beijing

Overall, the climatology of aerosol types over a period of almost two-decades (2001–2018) over Kanpur clearly shows a positive trend (statistically significant) of BB aerosol type in every season, a negative trend (statistically significant) of UI type in winter and pre-monsoon and a positive trend during monsoon and post-monsoon, and a negative trend (statistically significant) of DU type during pre-monsoon and monsoon (Fig. 5, Table 1). The DU type is not present in post-monsoon and winter. On the annual scale (Fig. 5e), BB and UI show positive trends over Kanpur while DU shows a negative trend. The seasonal trends are examined in order to be able to attribute the annual trends to changes in seasonal aerosol loading. This is necessary as both the study regions experience strong seasonal changes in aerosol amounts and types due to seasonal changes in natural processes and anthropogenic activities, and therefore, breaking down the annual trend into seasonal trends would enable a tracing of different sources of aerosols contributing to seasonal and annual trends. Over Beijing, UI aerosol type has a slight negative trend on annual scale during 2001–2018 whereas BB and DU aerosols exhibit a small positive trend (Fig. 5j). These annual trends are not statistically significant though (Table 1), in contrast to Kanpur where the trend in BB aerosol type is statistically significant. On a seasonal scale, the negative trend in UI aerosols over Beijing and the positive trend in BB aerosols are statistically significant during winter. The pattern of trend – increasing BB and decreasing UI – observed during winter also occurs in pre-monsoon, and DU shows a subtle positive trend in pre-monsoon. The scenario reverses in monsoon where BB shows a negative trend whereas UI exhibits a positive trend, both trends being statistically significant. The post-monsoon negative trend in UI aerosol type is statistically significant as opposed to the statistically insignificant positive trend in BB aerosol type. The inter-annual variation in aerosol types is

observed to be higher over Beijing than Kanpur during post-monsoon. The statistical significance of the trends estimated for 2001–2018 is found to have a low *p*-value ≤0.05 (meaning highly significant) at 95% confidence level in almost all of the trends on aerosol types and absorbing aerosol types on both seasonal and yearly time scales (Tables 1, 2).

The climatology and the trends observed in aerosol types are corroborated by the changes in volume concentration and their percentage contribution in fine (aerosols of radius < 1 μm), coarse (particles of radius > 1 μm) modes, and their total (Figs. 6, 7). The fine mode aerosol volume concentration over Kanpur has increased with statistically significant trends during the last 2-decades in all the seasons, and on the yearly scale (Fig. 6, Table 2). The increasing trends in fine mode aerosol volume concentrations are in tandem with the positive trends in UI and/or BB aerosol types, which are typically in fine mode. Likewise, the significantly negative trend of coarse mode volume concentration during pre-monsoon is consistent with the negative trend in dust aerosol type (Fig. 5). The percentage contribution of fine mode aerosols to the total volume concentration also shows a positive trend (Fig. 7) whereas the share of coarse mode aerosol to total volume shows a negative trend throughout the year, with both trends statistically significant (Table 2), which is consistent with the trends in aerosol types (Fig. 5, Table 1). Over Beijing, the fine, coarse and total aerosol volume concentrations all show negative trends on both annual and seasonal scales (Fig. 6), with the trends statistically significant during pre-monsoon and monsoon season (Table 2). In contrast to South Asian aerosols, over Beijing the percentage contribution of fine mode aerosols to total volume has negative trends during winter and pre-monsoon whereas it has positive trends during monsoon and post-monsoon (Fig. 7). On the yearly scale, it shows a negative trend (Fig. 7). The percentage contribution of coarse mode aerosols exhibits trends opposite to trends of fine mode's contribution (Fig. 7).

The linear depolarization ratio (LDR), a measure of shape and size of aerosol particles in the size distribution, can be used to distinguish the dominance of fine mode from coarse mode particles in the aerosol distribution. LDR is smaller for fine mode aerosols (which are mostly spherical) than coarse mode dust (and sea salt) particles which can be aspherical. Typical values of LDR for fine mode aerosols (from fossil fuel and biomass burning emissions) are in the 0.05–0.10 range whereas for dust particles LDR is higher (≥0.20 or even higher) (Ramachandran et al., 2020b). The seasonal and annual mean LDR over both Kanpur and Beijing are <0.30 (Fig. 8). On seasonal scale the LDR is <0.10 over Kanpur during post-monsoon and winter corroborating the dominance of fine mode aerosols whereas LDR is >0.10 going up to ~0.25 during pre-monsoon and monsoon seasons. The annual mean LDR values are close to 0.10. The LDR values over Beijing are <0.10 throughout the year except for pre-monsoon (Fig. 8). The LDR values exhibit decreasing trends over Kanpur during all the seasons (except for winter) and annually. Over Beijing LDR exhibits a decreasing trend during post-monsoon and winter. The LDR shows a statistically significant trend over Kanpur during monsoon facilitated by the statistically significant increasing (decreasing) trends of UI and BB (dust) aerosol types. The climatology and trend analysis of LDR over the IGP and NCP show that overall LDR values are lower, decreasing in general, and confirm that the fine (coarse) mode aerosols are increasing (decreasing).

The absorbing aerosol types are MBC and MIX only during post-monsoon and winter over Kanpur whereas during pre-monsoon and

Table 2

Details of statistical tests (*p*-values at 95% confidence level) for the trends in aerosol volume concentration in fine and coarse modes and their total over Kanpur and Beijing on seasonal and annual scales. Trends in percentage contribution of fine mode aerosols to total volume concentration, and coarse mode aerosols to total volume concentration are also given. p-values ≤0.05 are shown in boldface.

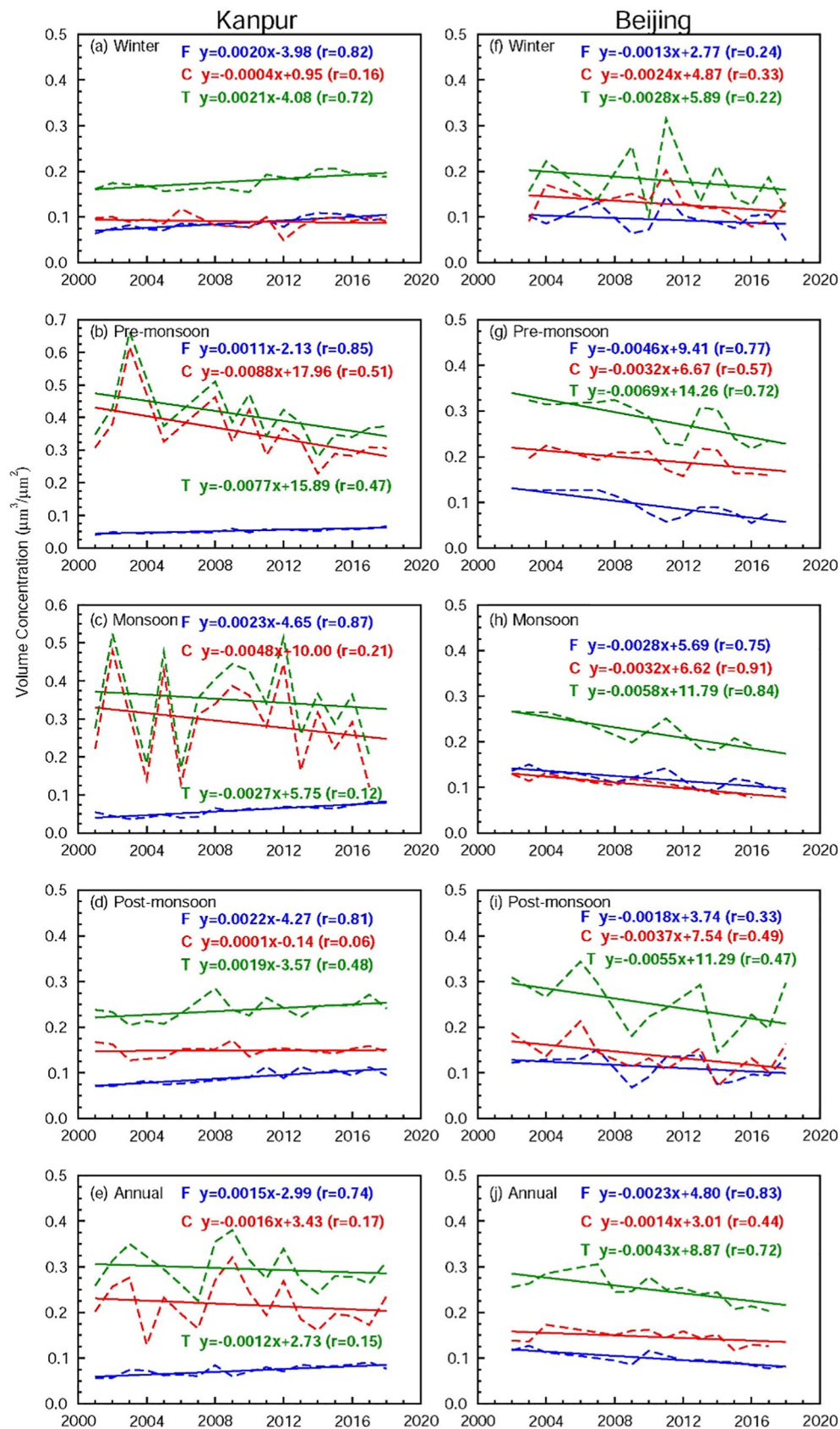| Season	Kanpur					Beijing				
	Fine	Coarse	Total	%Fine to Total	%Coarse to Total	Fine	Coarse	Total	%Fine to Total	%Coarse to Total
Kanpur										
Winter	**<0.01**	0.51	**<0.01**	**<0.01**	**<0.01**	0.41	0.26	0.47	0.81	0.81
Pre-monsoon	**<0.01**	**0.05**	0.07	**<0.01**	**<0.01**	**<0.01**	**0.04**	**<0.01**	**<0.01**	**<0.01**
Monsoon	**<0.01**	0.43	0.64	**<0.01**	**<0.01**	**<0.01**	**<0.01**	**<0.01**	0.08	0.08
Post-monsoon	**<0.01**	0.91	0.07	**0.01**	**0.01**	0.25	0.08	0.10	0.41	0.41
Annual	**<0.01**	0.46	0.52	**<0.01**	**<0.01**	**<0.01**	0.10	**<0.01**	0.08	0.08

Fig. 6. Seasonal and annual trends in volume concentration of aerosols ($\mu m^3/\mu m^2$) in fine mode (F), coarse mode (C) and total (T) over Kanpur and Beijing during 2001–2018 derived from the AERONET observations: left column for Kanpur [(a) winter, (b) pre-monsoon, (c) monsoon, (d) post-monsoon, and (e) annual], and right column for Beijing [(f) winter, (g) pre-monsoon, (h) monsoon, (i) post-monsoon and (j) annual]. The equations for the overall trend (2001–2018) in volume concentrations in fine (F), coarse (C) and total (T) are also given in each figure.
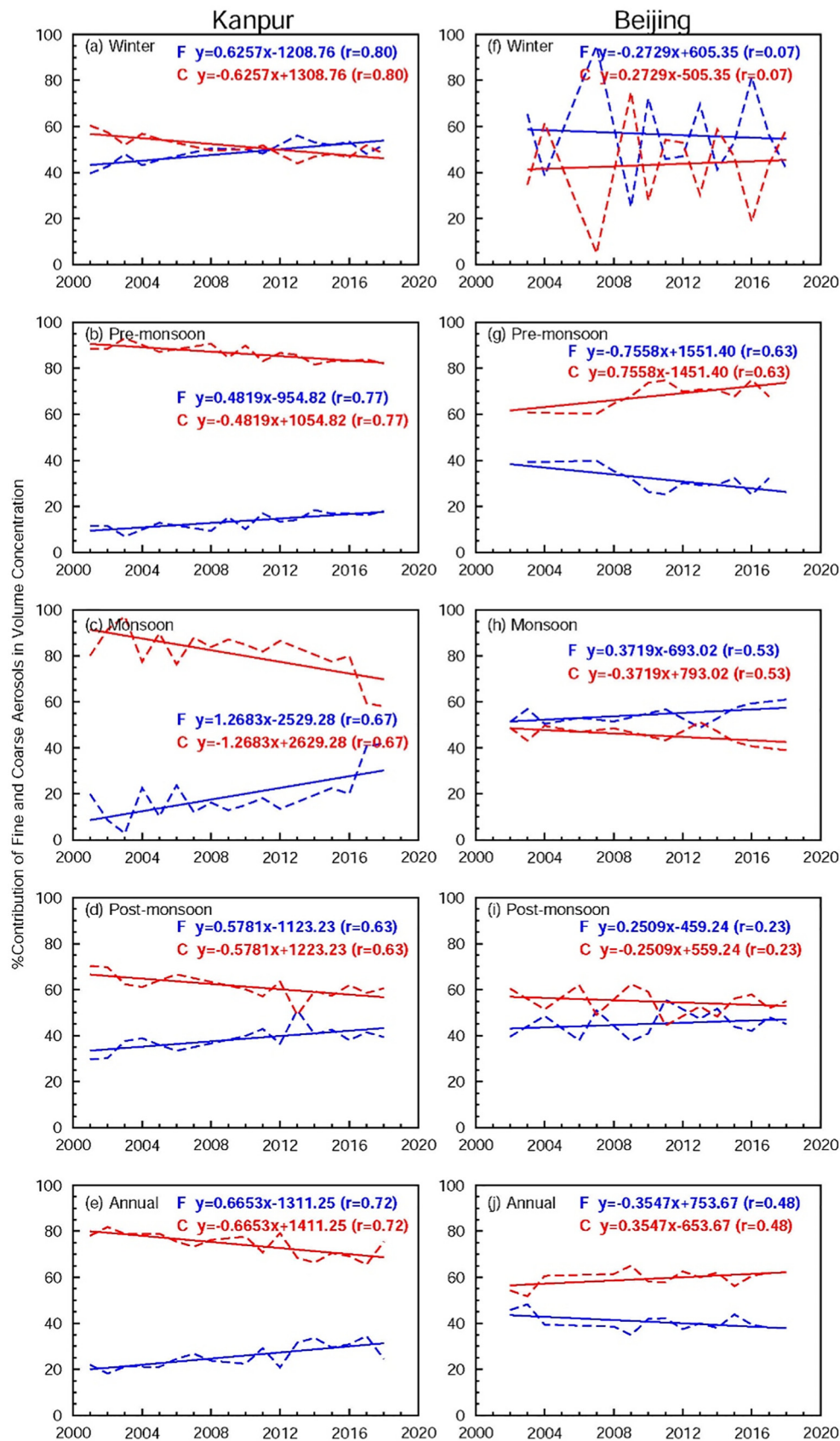
Fig. 7. Seasonal and annual percentage contributions of fine mode (F) and coarse mode (C) aerosols to the total volume concentrations (Fig. 6) and their trends over Kanpur and Beijing during 2001–2018: left column for Kanpur [(a) winter, (b) pre-monsoon, (c) monsoon, (d) post-monsoon, and (e) annual], and right column for Beijing [(f) winter, (g) pre-monsoon, (h) monsoon, (i) post-monsoon, and (j) annual]. The equations for the overall trend (2001–2018) for each mode are given in each figure.
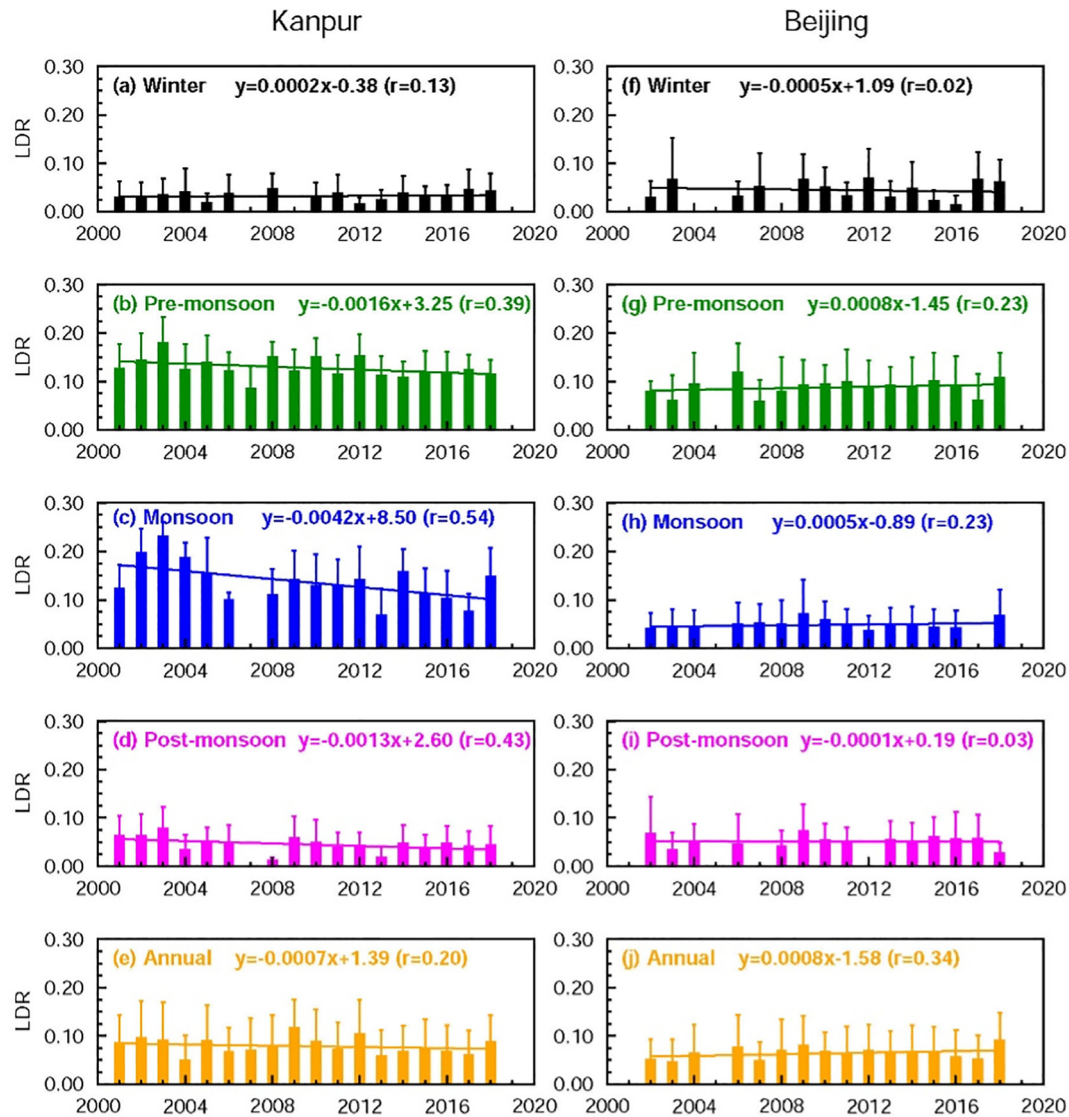
Fig. 8. Seasonal and annual mean linear depolarization ratio (LDR) of aerosols over Kanpur Beijing during 2002–2018 derived from the AERONET observations: left column for Kanpur [(a) winter, (b) pre-monsoon, (c) monsoon, (d) post-monsoon, and (e) annual], and right column for Beijing [(f) winter, (g) pre-monsoon, (h) monsoon, (i) post-monsoon, and (j) annual]. Vertical bars indicate ± 1σ (standard deviation) from the mean. Trend lines and the equations for the overall trend (2001–2018) for LDR are given at the top of each figure.

monsoon MDU is also present (Fig. 9) consistent with the aerosol types found (Fig. 5). The MBC shows an increasing trend throughout the year in all the seasons whereas the MIX absorbing aerosol type exhibits a decreasing trend during post-monsoon and winter over Kanpur in IGP, South Asia. The MDU, present only in pre-monsoon and monsoon, shows a decreasing trend which leads to an annually decreasing trend during the last two-decades over the IGP. The trends (increase/decrease) of MBC, MIX and MDU over Kanpur are statistically significant during the year except in post-monsoon of that of MBC (Fig. 9, Table 3). In contrast, over Beijing in East Asia, MBC shows a decreasing trend in all the seasons (except winter) and yearly, while the MIX type exhibits an increasing trend on seasonal and annual scales. The MDU absorbing aerosol type is present only during pre-monsoon and shows almost no trend on seasonal (pre-monsoon) as well as annual timescales. The decreasing trends of MBC over Beijing are statistically significant during pre-monsoon and post-monsoon seasons, and on yearly scale. The trends of MIX type which is increasing over Beijing in the last two-decades are statistically significant throughout the year (except in pre-monsoon when the decrease in MBC type is statistically significant (Table 3)). The trends in absorbing aerosol

types (Fig. 9) are consistent with the trends obtained on aerosol types (Fig. 5) and the volume concentrations in fine and coarse modes (Figs. 6, 7).

3.4. Discussion

The sixth assessment report released by the IPCC in 2021 states that our inadequate understanding of magnitudes and trends of atmospheric aerosols, particularly over Asia, is a major source of uncertainty in climate change (IPCC, 2021). For an accurate and better quantification of aerosol direct and indirect radiative effects and their climate impact not only the trends but also the magnitudes in aerosol types and absorbing aerosol types are crucial, especially over highly polluted aerosol source region such as Asia. One of the main factors that contributes to the uncertainty is especially the lack of knowledge on absorbing aerosols. However, quantitative determination and attribution of the atmospheric warming produced by these aerosol types has been difficult, especially due to a 50% uncertainty in their contribution to aerosol absorption (IPCC, 2013). AOD is directly proportional to aerosol loading and the size distribution of aerosol mass burden in atmospheric column; typically, in the aerosol size
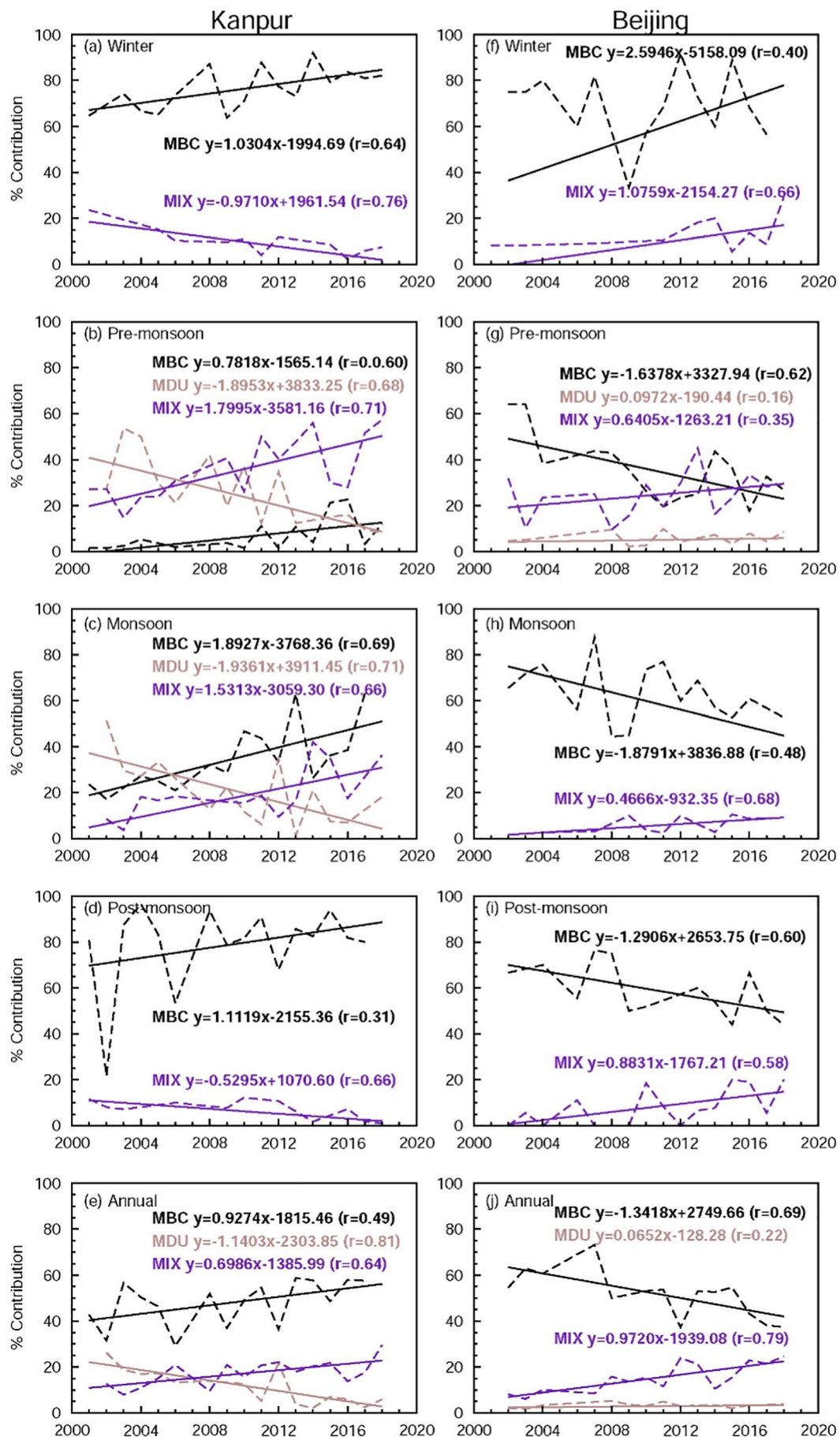
Table 3

Details of statistical tests (*p*-values at 95% confidence level) for the trends in absorbing aerosol types (Mostly BC (MBC), Mostly Dust (MDU) and Mixed (MIX)) over Kanpur and Beijing on seasonal and annual scales. p-values ≤ 0.05 are highlighted in boldface.

Season	Kanpur			Beijing		
	MBC	MDU	MIX	MBC	MDU	MIX
Winter	**<0.01**		**<0.01**	0.13		**0.01**
Pre-monsoon	**0.01**	**<0.01**	**<0.01**	**0.02**	0.58	0.21
Monsoon	**<0.01**	**<0.01**	**<0.01**	0.06		**<0.01**
Post-monsoon	0.25		**0.01**	**0.03**		**0.02**
Annual	**0.05**	**<0.01**	**<0.01**	**<0.01**	0.44	**<0.01**

distribution, number of fine mode aerosols are orders of magnitude higher than coarse mode particles. The aerosol size distribution plays a crucial role in determining the value of SSA as it is determined (whether high or low) by the ratio of the number of absorbing to scattering particles in a size distribution. Typically, the columnar content (AOD) over a region/location is dominated by the scattering aerosols (e.g., sulfate, SSA = 1.00) which are relatively more abundant in the atmosphere whereas the SSA, a measure of absorption capacity of aerosols in the atmosphere and related to chemical composition, is controlled/governed by the absorbing aerosols whose SSAs are lower (e.g., in particular BC, SSA = 0.19) even though their contribution to AOD is less than the other aerosol constituents. The relation between AOD and SSA is distinct is substantiated by the fact that when the aerosol loading in the atmosphere decreases AOD also decreases, however, a decrease in aerosol loading need not change the SSA as SSA is determined by the ratio of scattering to absorbing aerosols, as stated earlier. Thus, for any change in SSA to occur the composition of aerosol distribution (ratio of scattering to absorbing aerosols) should change whereas for any change in AOD the aerosol loading comprising scattering and absorbing aerosols should change (increase or decrease). Further, the relationship between AOD and aerosol radiative forcing (atmospheric warming) is linear, whereas the relation between SSA and atmospheric warming is non-linear; for example, the atmospheric warming increases by 10% for a 10% increase in AOD, but it increases by >20% for a 10% decrease in SSA from 0.99 to 0.89. It is imperative, therefore, that trends and quantification of absorbing aerosol types are quite crucial, which is the major focus of the present study, to reduce the uncertainty in the direct and indirect radiative effects and hence on climate. Developing effective mitigation options for climate change over Asia, a major aerosol hot spot, yet vulnerable and relatively poorly-studied region, requires a better quantification of the contributions of absorbing aerosol particles. In the present work, the magnitudes and trends in aerosol, and absorbing aerosol types are quantified accurately using high-quality ground-based observations on seasonal scales over Asia.

With an aim to address the public health concerns stringent air quality measures were introduced in 2008 over South Asia and East Asia (more stringent) since when the aerosol emissions have been changing. The reduction of sulfur dioxide (SO_2) and other pollutants including black carbon (BC) is seen to be more rapid over China than India (Li et al., 2017; Zheng et al., 2018), however, with significant differences in their rates of decrease – SO_2 emissions decreased by 62% and BC emissions decreased by 28% during 2010–2017 (Zheng et al., 2018; Kurokawa and Ohara, 2020; Kanaya et al., 2020). BC emissions in China were found to increase from early 2000s to 2010, which then started to fall mainly due to reductions in transport and industrial emissions rapidly accompanied with a slight decrease in residential emissions (Kurokawa and Ohara, 2020; Kanaya et al., 2020). The reductions in residential emissions were mainly caused by a decrease in emissions from biofuel consumption (Kurokawa and Ohara, 2020). In contrast, in India BC emissions showed positive trends

during the same period due to the growth of emissions from diesel vehicles and industry sector (Kurokawa and Ohara, 2020). In the transport sector, the increase in these emissions was smaller than the corresponding increase in fuel consumption because of implementation of emissions and fuel quality norms in India (Sadavarte and Venkataraman, 2014). The BB aerosol type exhibits statistically significant increasing trends in all seasons over Kanpur in the IGP (Fig. 5, Table 1) suggesting that biomass burning aerosols and associated precursor emissions have increased during the last two-decades over the IGP. This corroborates the results from a trend analysis of MODIS Aqua AODs over the IGP region which showed an increase in AOD of 0.0187 per year during the post-monsoon and 0.0168 per year during winter over the IGP during 2002–2016, which was attributed to a positive trend in agricultural fires during the same period as a major factor contributing to the trend, in addition to the increase in fossil fuel burning emissions (Jethva et al., 2019). The vegetation fires in South and Southeast Asian countries have shown a positive trend during 2002–2016 (Jethva et al., 2019; Vadrevu et al., 2019), however, there are no studies reporting trends or changes in biomass burning activities such as agro-residue/waste burning and forest fires over East Asia which might influence aerosol loading and composition. In the absence of such information, it is clear that the reduction in anthropogenic aerosol content (mainly sulfate, and BC) over Beijing resulted in a negative trend of MBC in all seasons. Thus, the seasonal trend analysis of aerosol types and absorbing aerosol types clearly illustrates that natural aerosols (mainly dust) decreased over the IGP and NCP during the last two decades. Further, the influence of changes in climatic factors (meteorology) leading to long term trends in aerosol characteristics was relatively small (e.g., Zhang et al., 2019). Therefore, it is clear from the study that the changing (positive/negative) trends in aerosols from urban/industrial and biomass burning emissions and the resultant absorbing aerosol types, BC and BC mixed with dust occur mainly due to the increase/decrease in emissions of anthropogenic aerosols and aerosol precursor gases.

4. Conclusions

The climatology and the trends on seasonal and annual time scales in aerosol types and absorbing aerosol types unavailable so far over two important regions, East Asia and South Asia are derived, by performing the first analysis of high quality time series of observations over a period of two-decades of the radiative- and climate-relevant columnar aerosol characteristics over Kanpur located in the Indo-Gangetic Plains (IGP) in South Asia and Beijing in the North China Plain (NCP) in East Asia, along with satellite observations to provide a broader regional perspective. An analysis of MODIS retrieved Ångström exponent (AE), spectral derivative of columnar aerosol optical depth (AOD), reveals that AE in the recent 5-year period (2014–2018) is higher than the first 5-year period (2001–2005) of the 21st century indicating that fine mode aerosols have increased over Asia in the last 2-decades. The increasing trends are statistically significant (at 95% confidence level) and robust over Kanpur and IGP in South Asia. The climatology of aerosol types, categorized as urban/industrial (UI), biomass burning (BB) and dust (DU), reveals that the aerosols are of UI and BB types over Kanpur in IGP during winter and post-monsoon, whereas DU is present only during pre-monsoon and monsoon. Overall, the BB aerosols show a positive trend, UI type exhibits a negative trend during winter and pre-monsoon and DU shows a negative trend during pre-monsoon and monsoon. On the annual scale, BB and UI aerosols show positive trends over Kanpur while DU shows a negative trend. Over Beijing in NCP, UI aerosols decrease on annual scale during 2001–2018 whereas BB aerosols exhibit a positive trend. The DU aerosols show a small positive trend, however, the annual trends during 2001–2018 are not statistically significant over Beijing for any aerosol type, in contrast to Kanpur where the trend in BB aerosol type is statistically significant. On a seasonal scale, however, over

Fig. 9. Seasonal and annual trends in absorbing aerosol types [classified as Mostly BC(MBC), Mostly Dust (MDU), and Mixed (MIX)] over the IGP and NCP during 2001–2018: left column for Kanpur [(a) winter, (b) pre-monsoon, (c) monsoon, (d) post-monsoon, and (e) annual], and right column for Beijing [(f) winter, (g) pre-monsoon, (h) monsoon and (i) post-monsoon, and (j) annual]. Trend lines and the equations for the overall trend (2001–2018) for the respective absorbing aerosol type are given in each figure.

Beijing the positive trend in UI aerosols and the negative trend in BB aerosols are statistically significant during winter, and further the negative trend in post-monsoon in UI aerosols is statistically significant as opposed to the positive trend in BB aerosols. The climatology and trend analysis of aerosol volume concentrations in fine and coarse modes, and linear depolarization (LDR) confirm that fine (coarse) mode aerosols are increasing (decreasing) over IGP and NCP.

The absorbing aerosol types, classified as Mostly BC (MBC), Mostly Dust (MDU) and Mixed (MIX) substantiates the findings on the observed aerosol types over the IGP and the NCP. MBC and MIX are the only two absorbing aerosol types in post-monsoon and winter over the IGP, and MDU is present only during pre-monsoon and monsoon. MBC shows a positive trend throughout the year while MIX aerosols exhibit a negative trend in post-monsoon and winter. MDU shows a negative trend over the IGP. The positive and/or negative trends of MBC, MIX and MDU over Kanpur in the IGP are statistically significant during the year except for MBC in post-monsoon. The trend of MIX which is increasing over Beijing in the NCP in the last two-decades is statistically significant throughout the year (except in pre-monsoon when the decrease in MBC type is statistically significant). The MDU aerosols are present only during pre-monsoon over the NCP and shows no trend during this season as well on the annual scale. The seasonal trends in aerosol types and absorbing aerosol types occur mainly due to the increase/decrease in emissions of anthropogenic aerosols and aerosol precursor gases, and not due to natural and climatic factors (meteorology) as the changes in natural aerosols and climatic factors leading to long term trends in aerosol characteristics are relatively small. These findings from the first-of-its-kind analyses on the hitherto unavailable climatology and trends in aerosols and absorbing aerosols over two global aerosol hotspots will be crucial in model simulations to better decipher the aerosol-climate interactions over Asia, and undertake potential mitigation strategies to help reduce their impacts on climate, ecosystems and human health.

Author contributions

SR designed the study in consultation with MR. SR performed the analysis and wrote the paper. Both authors reviewed and edited the paper.

Data availability

All data used in the manuscript are publicly available at https://giovanni.gsfc.nasa.gov/giovanni/ and https://aeronet.gsfc.nasa.gov/ respectively.

Declaration of competing interest

The authors declare that they have no known competing financial interests or personal relationships that could have appeared to influence the work reported in this paper.

References

An, Z., Huang, R.-J., Zhang, R., Tie, X., Li, G., Cao, J., Zhou, W., Shi, Z., Han, Y., Gu, Z., Ji, Y., 2019. Severe haze in northern China: a synergy of anthropogenic emissions and atmospheric processes. Proc. Natl. Acad. Sci. 116, 8657–8666. https://doi.org/10.0173/pnas.1900125116.

Che, H., Qi, B., Zhao, H., Xia, X., Eck, T.F., Goloub, P., Dubovik, O., Estelles, V., Cuevas-Agulló, E., Blaerl, L., Wu, Y., Zhu, J., Du, R., Wang, Y., Wang, H., Gui, K., Yu, J., Zheng, Y., Sun, T., Chen, Q., Shi, G., Zhang, X., 2018. Aerosol optical properties and direct radiative forcing based on measurements from the China Aerosol Remote Sensing Network (CARSNET) in eastern China. Atmos. Chem. Phys. 18, 405–425. https://doi.org/10.5194/acp18-405-2018.

Che, H., Xia, X., Zhao, H., Dubovik, O., Holben, B.N., Goloub, P., Cuevas-Agulló, E., Estelles, V., Wang, Y., Zhu, J., Qi, B., Gong, W., Yang, H., Zhang, R., Yang, L., Chen, J., Wang, H., Zheng, Y., Gui, K., Zhang, X., Zhang, X., 2019. Spatial distribution of aerosol microphysical and optical properties and direct radiative effect from the China aerosol remote sensing network. Atmos. Chem. Phys. 19, 11843–11864. https://doi.org/10.5194/acp-19-11843-2019.

Dubovik, O., Smirnov, A., Holben, B.N., King, M.D., Kaufman, Y.J., Eck, T.F., Schuster, I., 2000. Accuracy assessments of aerosol optical properties retrieved from aerosol robotic network (AERONET) sun and sky radiance measurements. J. Geophys. Res. 105, 9791–9806.

Dubovik, O., Holben, B., Eck, T.F., Smirnov, A., Kaufman, Y.J., King, M.D., Tanre, D., Slutsker, I., 2002. Variability of absorption and optical properties of key aerosol types observed in worldwide locations. J. Atmos. Sci. 59, 590–608.

Eck, T.F., Holben, B.N., Sinyuk, A., Pinker, R.T., Goloub, P., Chen, H., Chatenet, B., Li, Z., Singh, R.P., Tripathi, S.N., Reid, J.S., Giles, D.M., Dubovik, O., O'Neill, N.T., Smirnov, A., Wang, P., Xia, X., 2010. Climatological aspects of the optical properties of fine/coarse mode aerosol mixtures. J. Geophys. Res. 115, D19205. https://doi.org/10.1029/2010JD014002.

Fan, H., Zhao, C., Yang, Y., 2020. A comprehensive analysis of the spatio-temporal variation of urban air pollution in China during 2014–2018. Atmos. Env. 220. https://doi.org/10.1016/j.atmosenv.2019.117066.

Giles, D.M., Holben, B.N., Eck, T.F., Sinyuk, A., Smirnov, A., Slutsker, I., Dickerson, R.R., Thompson, A.M., Schafer, J.S., 2012. An analysis of AERONET aerosol absorption properties and classifications representative of aerosol source regions. J. Geohpys. Res. 117, D17203. https://doi.org/10.1029/2012JD018127.

Hoegh-Guldberg, O., Jacob, D., Taylor, M., Bindi, M., Brown, S., Camilloni, I., Diedhiou, A., Djalante, R., Ebi, K.L., Engelbrecht, F., Guiot, J., Hijioka, Y., Mehrotra, S., Payne, A., Seneviratne, S.I., Thomas, A., Warren, R., Zhou, G., 2018. Impacts of 1.5°C global warming on natural and human systems. In: Masson-Delmotte, V., Zhai, P., Pörtner, H.-O., Roberts, D., Skea, J., Shukla, P.R., Pirani, A., Moufouma-Okia, W., Péan, C., Pidcock, R., Connors, S., Matthews, J.B.R., Chen, Y., Zhou, X., Gomis, M.I., Lonnoy, E., Maycock, T., Tignor, M., Waterfield, T. (Eds.), Global Warming of 1.5°C. An IPCC Special Report on the Impacts of Global Warming of 1.5°C Above Pre-industrial Levels and Related Global Greenhouse Gas Emission Pathways, in the Context of Strengthening the Global Response to the Threat of Climate Change, Sustainable Development, and Efforts to Eradicate Poverty. IPCC, pp. 175–312.

Holben, B.N., Tanré, D., Smirnov, A., Eck, T.F., Slutsker, I., Abuhassan, N., Newcomb, W.W., Schafer, J.S., Chatenet, B., Lavenu, F., Kaufman, Y.J., Castle, J.V., Setzer, A., Markham, B., Clark, D., Frouin, R., Halthore, R., Karneli, A., O'Neill, N.T., Pietras, C., Pinker, R.T., Voss, K., Zibordi, G., 2001. An emerging ground-based aerosol climatology: aerosol optical depth from AERONET. J. Geophys. Res. 106, 12067–12097.

IPCC, 2013. In: Stocker, T.F., Qin, D., Plattner, G.-K., Tignor, M., Allen, S.K., Boschung, J., Nauels, A., Xia, Y., Bex, V., Midgley, P.M. (Eds.), Summary for Policymakers in Climate Change 2013: The Physical Science Basis. Contribution of Working Group I to the Fifth Assessment Report of the Intergovernmental Panel on Climate Change. Cambridge Univ. Press, Cambridge, UK. and NY, USA, pp. 1–33.

IPCC, 2021. Summary for policymakers. In: Masson-Delmotte, V., Zhai, P., Pirani, A., Connors, S.L., Péan, C., Berger, S., Caud, N., Chen, Y., Goldfarb, L., Gomis, M.I., Huang, M., Leitzell, K., Lonnoy, E., Matthews, J.B.R., Maycock, T.K., Waterfield, T., Yelekçi, O., Yu, R., Zhou, B. (Eds.), Climate Change 2021: The Physical Science Basis. Contribution of Working Group I to the Sixth Assessment Report of the Intergovernmental Panel on Climate Change. Cambridge University Press In Press.

Jethva, H., Torres, O., Field, R.D., Lyapustin, A., Gautam, R., Kayetha, V., 2019. Connecting crop productivity, residue fires, and air quality over northern India. Sci. Rep. 9. https://doi.org/10.1038/s41598-019-52799-x.

Kanaya, Y., Yamaji, K., Miyakawa, T., Taketani, F., Zhu, C., Choi, Y., Komazaki, Y., Ikeda, K., Kondo, Y., Klimont, Z., 2020. Rapid reduction in black carbon emissions from China: evidence from 2009–2019 observations on Fukue Island, Japan. Atmos. Chem. Phys. 20, 6339–6356. https://doi.org/10.5194/acp-20-6339-2020.

Kedia, S., Ramachandran, S., Tripathi, S.N., Holben, B., 2014. Quantification of aerosol type, and sources of aerosols over the Indo-Gangetic Plain. Atmos. Environ. 98, 607–619.

Kirillova, E.N., Marinoni, A., Bonasoni, P., Vuillermoz, E., Facchini, M.C., Fuzzi, S., Decesari, S., 2016. Light absorption properties of brown carbon in the high Himalayas. J. Geophys. Res. 121. https://doi.org/10.1002/2016JD025030.

Kurokawa, J., Ohara, T., 2020. Long-term historical trends in air pollutant emissions in Asia: regional emission inventory in ASia (REAS) version 3. Atmos. Chem. Phys. 20, 12761–12793. https://doi.org/10.5194/acp-20-12761-2020.

Levy, R.C., Mattoo, S., Munchak, L.A., Remer, L.A., Sayer, A.M., Patadia, F., Hsu, N.C., 2013. The collection 6 MODIS aerosol products over land and ocean. Atmos. Meas. Tech. 6, 2989–3034.

Li, C., McLinden, C., Fioletov, V., Krotkov, N., Carn, S., Joiner, J., Streets, D., He, H., Ren, X., Li, Z., Dickerson, R.R., 2017. India is overtaking China as the world's largest emitter of anthropogenic sulfur dioxide. Sci. Rep. 7, 14304.

Li, W., Shao, L., Wang, W., Li, H., Wang, X., Li, Y., Li, W., Jones, T., Zhang, D., 2020. Air quality improvement in response to intensified control strategies in Beijing during 2013–2019. Sci. Total Environ. 744 (140776), 2020.

Meng, J., Yang, H., Yi, K., Liu, J., Guan, D., Liu, Z., Mi, Z., Coffman, D.M., Wang, X., Zhong, Q., Huang, T., Meng, W., Tao, S., 2019. The slowdown in global air-pollutant emission growth and driving factors. One Earth 1, 136–148.

Myhre, G., Samset, B.H., Schulz, M., Balkanski, Y., Bauer, S., Berntsen, T.K., Bian, H., Bellouin, N., Chin, M., Diehl, T., Easter, R.C., Feichter, J., Ghan, S.J., Hauglustine, D., Iversen, T., Kinne, S., Kirkevåg, A., Lamarque, J.-F., Lin, G., Liu, X., Lund, M.T., Luo, G., Ma, X., van Noije, T., Penner, J.E., Rasch, P.J., Ruiz, A., Seland, Ø., Skeie, R.B., Stier, P., Takemura, T., Tsigardis, K., Wang, P., Wang, Z., Xu, L., Yu, H., Yu, F., Yoon, J.-H., Zhang, K., Zhang, H., Zhou, C., 2013. Radiative forcing of the direct effect from AeroCom phase II simulations. Atmos. Chem. Phys. 13, 1853–1877. https://doi.org/10.5194/acp-13-1853-2013.

Myhre, G., Aas, W., Cherian, R., Collins, W., Faluvegi, G., Flanner, M., Forster, P., Hodneborg, Ø., Klimont, Z., Lund, M.T., Mülmenstädt, J., Myhre, C.L., Olivié, D., Prather, M., Quaas, J., Samset, B.H., Schnell, J.L., Schultz, M., Shindell, D., Skeie, R.B., Takemura, T., Tsyro, S., 2017. Multi-model simulations of aerosol and ozone radiative forcing due to anthropogenic emission changes during the period 1990–2015. Atmos. Chem. Phys. 17, 2709–2720. https://doi.org/10.5194/acp-17-2709-2017.

Ramachandran, S., Rupakheti, M., 2020. Year-round aerosol characteristics and radiative effects in the South Asian pollution outflow over a background site in the Maldives. Atmos. Env. 240. https://doi.org/10.1016/j.atmosenv.2020.117813.

O'Neill, N.T., Eck, T.F., Smirnov, A., Holben, B.N., Thulasiraman, S., 2003. Spectral discrimination of coarse and fine mode optical depth. J. Geophys. Res. 108. https://doi.org/10.1029/2002JD002975.

Ramachandran, S., Kedia, S., Sheel, V., 2015. Spatiotemporal characteristics of aerosols in India: observations and model simulations. Atmos. Environ. 116, 225–244.

Ramachandran, S., Rupakheti, M., Lawrence, M., 2020a. Aerosol-induced atmospheric heating rate decreases over south and East Asia as a result of changing content and composition. Sci. Rep. 10, 20091. https://doi.org/10.1038/s41598-020-76936-z.

Ramachandran, S., Rupakheti, M., Lawrence, M.G., 2020b. Black carbon dominates the aerosol absorption over the Indo-Gangetic plain and the Himalayan foothills. Environ. Int. 142, 105814. https://doi.org/10.1016/j.envint.2020.105814.

Ramachandran, S., Rupakheti, M., Cherian, R., Lawrence, M.G., 2022. Climate benefits of cleaner energy transitions in East and South Asia through black carbon reduction. Front. Environ. Sci. https://doi.org/10.3389/fenvs.2022.842319.

Rupakheti, D., Kang, S., Rupakheti, M., Cong, Z., Panday, A.K., Holben, B.N., 2019. Identification of absorbing aerosol types at a site in the northern edge of Indo-Gangetic Plain and a polluted valley in the foothills of the central Himalaya. Atmos. Res. 223, 15–23.

Russell, P.B., Bergstrom, R.W., Shinozuka, Y., Clarke, A.D., DeCarlo, P.F., Jimenez, J.L., Livingston, J.M., Redemann, J., Dubovik, O., Strawa, A., 2010. Absorption angstrom exponent in AERONET and related data as an indicator of aerosol composition. Atmos. Chem. Phys. 10, 1155–1169.

Russell, P.B., Kacenelenbogen, M., Livingston, J.M., Haekamp, O.P., Burton, S.P., Shuscter, G.L., Johnson, M.S., Knobelspiesse, K.D., Redemann, J., Ramachandran, S., Holben, B., 2014. A multiparameter aerosol classification method and its application to retrievals from spaceborne polarimetry. J. Geophys. Res. 119, 9838–9863.

Sadavarte, P., Venkataraman, C., 2014. Trends in multi-pollutant emissions from a technology-linked inventory for India: I. Industry and transport sectors. Atmos. Environ. 99, 353–364.

Samset, B.H., Lund, M.T., Bollasina, M., Myhre, G., Wilcox, L., 2019. Emerging Asian aerosol patterns. Nat. Geosci. 12, 582–586.

Sayer, A.M., Hsu, N.C., Lee, J., Kim, W.V., Dutcher, S.T., 2019. Validation, stability, and consistency of MODIS collection 6.1 and VIIRS version 1 deep blue aerosol data over land. J. Geophys. Res. 124, 4658–4688. https://doi.org/10.1029/2018JD029598.

Shindell, D.T., Lamarque, J.-F., Schulz, M., Flanner, M., Jiao, C., Chin, M., Young, P.J., Lee, Y.H., Rotstayn, L., Mahowald, N., Milly, G., Faluvegi, G., Balkanski, Y., Collins, W.J., Conley, A.J., Dalsoren, S., Easter, R., Ghan, S., Horowitz, L., Liu, X., Nagashima, T., Naik, V., Rumbold, S.T., Skeie, R., Sudo, K., Szopa, S., Takemura, T., Voulgarakis, A., Yoon, J.-H., Lo, F., 2013. Radiative forcing in the ACCMIP historical and future climate simulations. Atmos. Chem. Phys. 13, 2939–2974.

UNEP, 2019. Air pollution in Asia and the Pacific: Science-based solutions. United Nations Environment Programme (UNEP) 250 pp.

Vadrevu, K.P., Lasko, K., Giglio, L., Schroeder, W., Biswas, S., Justice, C., 2019. Trends in vegetation fires in south and southeast Asian countries. Sci. Rep. 9. https://doi.org/10.1038/s41598-019-43940-x.

Xie, C., He, Y., Lei, L., Zhou, W., Liu, J., Wang, Q., Xu, W., Qiu, Y., Zhao, J., Sun, J., Li, L., Li, M., Zhou, Z., Fu, P., Wang, Z., Sun, Y., 2020. Contrasting mixing state of black carbon-containing particles in summer and winter in Beijing. Environ. Poll. 263 10.106/j.envpol.2020.114455.

Yang, X., Zhao, C., Yang, Y., Fan, H., 2021a. Long-term multi-source data analysis about the characteristics of aerosol optical properties and types over Australia. Atmos. Chem. Phys. 21, 3803–3825. https://doi.org/10.5194/acp-21-3803-2021.

Yang, X., Zhao, C., Wang, Q., Cong, Z., Yang, X., Fan, H., 2021b. Aerosol characteristics at the three poles of the earth as characterized by cloud-aerosol Lidar and infrared pathfinder satellite observations. Atmos. Chem. Phys. 21, 4849–4868. https://doi.org/10.5194/acp-21-4849-2021.

Zhang, Q., Zheng, Y., Tong, D., Shao, M., Wang, S., Zhang, Y., Xu, X., Wang, J., He, H., Liu, W., Ding, Y., Lei, Y., Li, J., Wang, Z., Zhang, X., Wang, Y., Cheng, J., Liu, Y., Geng, G., Hong, C., Li, M., Liu, F., Zheng, B., Cao, J., Ding, A., Gao, J., Fu, Q., Hua, J., Liu, B., Liu, Z., Yang, F., He, K., Hao, J., 2019. Drivers of improved PM2.5 air quality in China from 2013 to 2017. PNAS https://doi.org/10.1073/pnas.1907956116.

Zhao, H., Che, H., Ma, Y., Xia, X., Wang, Y., Wang, P., Wu, X., 2015. Temporal variability of the visibility, particulate matter mass concentration and aerosol optical properties over an urban site in Northeast China. Atmos. Res. 166, 204–212. https://doi.org/10.1016/j.atmosres.2015.07.003.

Zhao, C., Yang, Y., Fan, H., Huang, J., Fu, Y., Zhang, X., Kang, S., Cong, Z., Letu, H., Menenti, M., 2020. Aerosol characteristics and impacts on weather and climate over the Tibetan Plateau. Nat. Sci. Rev. 7, 492–495. https://doi.org/10.1093/nsr/nwz184.

Zheng, C., Zhao, C., Zhu, Y., Wang, Y., Shi, X., Wu, X., Chen, T., Wu, F., Qiu, Y., Yang, Y., Fan, H., 2017. Analysis of influencial factors for the relationship between PM2.5 and AOD in Beijing. Atmos. Chem. Phys. 17, 13473–13489. https://doi.org/10.5194/acp-17-13473-2017.

Zheng, B., Tong, D., Li, M., Liu, F., Hong, C., Geng, C., Li, H., Li, X., Peng, L., Qi, J., Yan, L., Zhang, Y., Zhao, H., Zheng, Y., He, K., Zhang, Q., 2018. Trends in China's anthropogenic emissions since 2010 as the consequence of clean air actions. Atmos. Chem. Phys. 18, 14095–14111.